Available online at www.sciencedirect.com
ScienceDirect
PHYTOCHEMISTRY
Phytochemistry 68 (2007) 1957–1974
www.elsevier.com/locate/phytochem

Expression of cinnamyl alcohol dehydrogenases and their putative homologues during *Arabidopsis thaliana* growth and development: Lessons for database annotations?

Sung-Jin Kim [a], Kye-Won Kim [a], Man-Ho Cho [a], Vincent R. Franceschi [b,✠], Laurence B. Davin [a], Norman G. Lewis [a,*]

[a] *Institute of Biological Chemistry, Washington State University, Pullman, WA 99164-6340, USA*
[b] *School of Biological Sciences, Washington State University, Pullman, WA 99164-4236, USA*

Received 31 October 2006; received in revised form 29 January 2007
Available online 27 April 2007

Abstract

A major goal currently in *Arabidopsis* research is determination of the (biochemical) function of each of its ~27,000 genes. To date, however, ⩽12% of its genes actually have known biochemical roles. In this study, we considered it instructive to identify the gene expression patterns of nine (so-called AtCAD1–9) of 17 genes originally annotated by The Arabidopsis Information Resource (TAIR) as cinnamyl alcohol dehydrogenase (CAD, EC 1.1.1.195) homologues [see Costa, M.A., Collins, R.E., Anterola, A.M., Cochrane, F.C., Davin, L.B., Lewis N.G., 2003. An *in silico* assessment of gene function and organization of the phenylpropanoid pathway metabolic networks in *Arabidopsis thaliana* and limitations thereof. Phytochemistry 64, 1097–1112.]. In agreement with our biochemical studies in vitro [Kim, S.-J., Kim, M.-R., Bedgar, D.L., Moinuddin, S.G.A., Cardenas, C.L., Davin, L.B., Kang, C.-H., Lewis, N.G., 2004. Functional reclassification of the putative cinnamyl alcohol dehydrogenase multigene family in *Arabidopsis*. Proc. Natl. Acad. Sci. USA 101, 1455–1460.], and analysis of a double mutant [Sibout, R., Eudes, A., Mouille, G., Pollet, B., Lapierre, C., Jouanin, L., Séguin A., 2005. *Cinnamyl Alcohol Dehydrogenase-C* and *-D* are the primary genes involved in lignin biosynthesis in the floral stem of *Arabidopsis*. Plant Cell 17, 2059–2076.], both AtCAD5 (At4g34230) and AtCAD4 (At3g19450) were found to have expression patterns consistent with development/formation of different forms of the lignified vascular apparatus, e.g. lignifying stem tissues, bases of trichomes, hydathodes, abscission zones of siliques, etc. Expression was also observed in various non-lignifying zones (e.g. root caps) indicative of, perhaps, a role in plant defense. In addition, expression patterns of the four CAD-like homologues were investigated, i.e. AtCAD2 (At2g21730), AtCAD3 (At2g21890), AtCAD7 (At4g37980) and AtCAD8 (At4g37990), each of which previously had been demonstrated to have low CAD enzymatic activity in vitro (relative to AtCAD4/5) [Kim, S.-J., Kim, M.-R., Bedgar, D.L., Moinuddin, S.G.A., Cardenas, C.L., Davin, L.B., Kang, C.-H., Lewis, N.G., 2004. Functional reclassification of the putative cinnamyl alcohol dehydrogenase multigene family in *Arabidopsis*. Proc. Natl. Acad. Sci. USA 101, 1455–1460.]. Neither AtCAD2 nor AtCAD3, however, were expressed in lignifying tissues, with the latter being found mainly in the meristematic region and non-lignifying root tips, i.e. indicative of involvement in biochemical processes unrelated to lignin formation. By contrast, AtCAD7 and AtCAD8 [surprisingly now currently TAIR-annotated as probable mannitol dehydrogenases, but for which there is still no biochemical or other evidence for same] displayed gene expression patterns largely resembling those of AtCAD4/5, i.e. indicative perhaps of a quite minor role in monolignol/lignin formation. Lastly, AtCAD1 (At1g72680), AtCAD6 (At4g37970) and AtCAD9 (At4g39330), which lacked detectable CAD catalytic activities in vitro, were also expressed predominantly in vascular (lignin-forming) tissues. While their actual biochemical roles remain unknown, definition of their expression patterns, nevertheless, now begins to provide useful insights into potential biochemical/physiological functions, as well as the cell types in which they are expressed.

Abbreviations: CAD, cinnamyl alcohol dehydrogenase; CWR, cell-wall residue; G, guaiacyl; GUS, β-glucuronidase; S, syringyl; SAD, sinapyl alcohol dehydrogenase; WT, wild type.

* Corresponding author. Tel.: +1 509 335 2682; fax: +1 509 335 8206.
E-mail address: lewisn@wsu.edu (N.G. Lewis).

✠ Deceased.

doi:10.1016/j.phytochem.2007.02.032

These data thus indicate that the CAD metabolic network is composed primarily of AtCAD4/5 and may provisionally, to a lesser extent, involve AtCAD7/8 based on in vitro catalytic properties and (promoter regions selected to obtain) representative gene expression patterns. This analysis has, therefore, enabled us to systematically map out *bona fide* CAD gene involvement in both the assembly and differential emergence of the various component parts of the lignified vascular apparatus in *Arabidopsis*, as well as those having other (e.g. putative plant defense) functions. The data obtained also further underscore the ongoing difficulties and challenges as regards current limitations in gene annotations versus actual determination of gene function. This is exemplified by the annotation of AtCAD2, 3 and 6–9 as purported mannitol dehydrogenases, when, for example, no in vitro studies have been carried out to establish such a function biochemically. Such annotations should thus be discontinued in the absence of reliable biochemical and/or other physiological confirmation. In particular, AtCAD2, 3, 6 and 9 should be designated as dehydrogenases of unknown function. Just as importantly, the different patterns of gene expression noted during distinct phases of growth and development in specific cells/tissues gives insight into the study of the roles that these promoters have.

Keywords: *Arabidopsis thaliana*; Cruciferae; Cinnamyl alcohol dehydrogenase; Cinnamyl alcohol dehydrogenase homologues; Mannitol dehydrogenase homologues; Lignin; Metabolic networks; GUS; Bioinformatics; Gene annotation

1. Introduction

The TAIR-annotated cinnamyl alcohol dehydrogenase (CAD, EC 1.1.1.195) gene family in *Arabidopsis* putatively encoded a seventeen-member class of NADPH-dependent enzymes (Costa et al., 2003; Kim et al., 2004). This 17-member annotation was originally made based on an initial database analysis of the *A. thaliana* genome, even though eight of the genes had essentially no homology (~0.9–1.6% similarity, Kim et al., 2004) to previously established *bona fide Nicotiana tabacum* (Knight et al., 1992) and *Pinus taeda* (Anterola et al., 2002) CAD's. Indeed, these eight genes in question encode proteins whose physiological functions are still uncertain at present, in contrast to at least one report of a related tobacco homologue which was described as a CAD involved in lignification (Damiani et al., 2005). However, definitive proof for such a role in lignification is lacking.

In this study, we have comprehensively examined gene expression patterns of the remaining nine-membered TAIR-annotated *bona fide* CAD and CAD homologue family in *Arabidopsis*. This was in order to systematically begin to establish further the actual gene networks involved in forming the various component parts of the (lignified) vascular apparatus, as well as in helping identify those potentially having other functions, such as defense.

The nine putative CAD's displayed various levels of homology to the tobacco CAD (Knight et al., 1992) (~57–83% similarity and ~46–77% identity). At the beginning of our study, these could be conveniently classified into three groups, based on both homology and biochemical properties in vitro, i.e. AtCAD4 (At3g19450) and 5 (At4g34230) (74 to ~83% similarity), AtCAD2 (At2g21730), AtCAD3 (At2g21890), AtCAD7 (At4g37980) and AtCAD8 (At4g37990) (61–65% similarity), as well as AtCAD1 (At1g72680), AtCAD6 (At4g37970) and AtCAD9 (At4g39330) (57–66% similarity) (Costa et al., 2003; Kim et al., 2004).

More importantly, a detailed determination of the kinetic parameters of the recombinant proteins (AtCAD1–9) in vitro established that AtCAD4 and 5 were the catalytically most active, being able to convert the various phenylpropenyl aldehyde derivatives **1**–**5** into the corresponding monolignols **6**–**10** (Fig. 1). AtCAD5 and AtCAD4 differ substantially, however, in their relative abilities to utilize sinapyl aldehyde (**5**) as substrate, with the former ~270-fold more efficient than AtCAD4 (Kim et al., 2004). Additionally, we have since recently demonstrated through X-ray crystal structure analysis that AtCAD4 and AtCAD5 exist in dimeric form, with both proteins containing structural Zn^{2+} and catalytic Zn^{2+} ions per subunit. Both AtCAD4 and AtCAD5 belong to the medium chain dehydrogenase/reductase (MDR) superfamily (Youn et al., 2006), and appear to have a fairly tight substrate binding pocket for the substrates **1**–**5**. By contrast, in terms of catalytic activity, AtCAD2, 3, 7 and 8 had much lower levels of CAD activity, with AtCAD1, 6 and 9 being inactive in our hands (Kim et al., 2004). These kinetic data, together with that of various knockout analyses, thus suggested that the *Arabidopsis* CAD metabolic network was potentially composed primarily of two genes (AtCAD4 and AtCAD5), with four others (AtCAD2, 3, 7, and 8) encoding proteins of more moderate CAD-like activity. Based on the experimentally determined kinetic data obtained for AtCAD2, 3, 7 and 8 (i.e. higher K_m's and lower k_{cat} values relative to AtCAD4/5), however, alternative and/or bifunctional metabolic roles could not be excluded.

In this context, it is quite noteworthy that the putative biochemical/physiological functions of the previously annotated cinnamyl alcohol dehydrogenase homologues (AtCAD2, 3, 6–9) have also recently been re-designated as probable/putative mannitol dehydrogenases in the TIGR database annotations (as of October 26, 2006). Such annotations are curious given that, to our knowledge, none of these specific enzymes have been demonstrated to catalyze these conversions via biochemical assays in vitro. Thus, some additional clarification and discussion are needed on this matter.

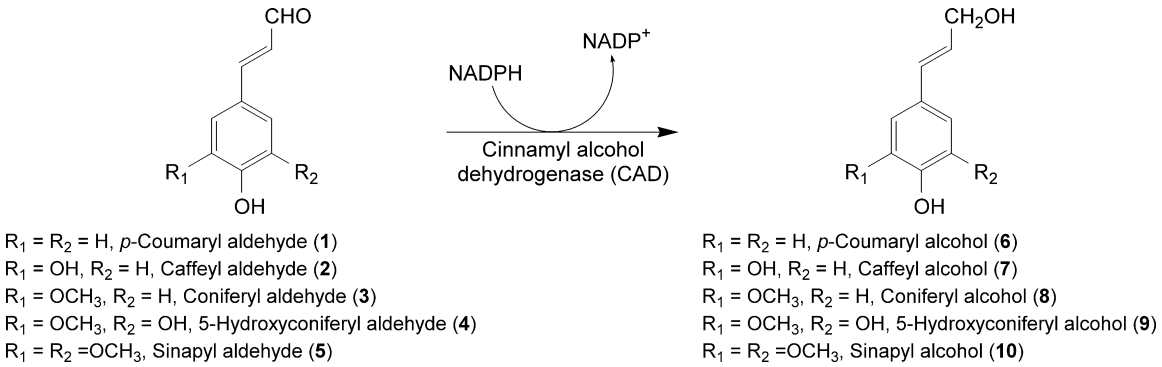

Fig. 1. Possible CAD substrates (**1**–**5**) and products (**6**–**10**).

In 1992, two inducible defense genes from *A. thaliana*, *ELI3-1* (*AtCAD7*) and *ELI3-2* (*AtCAD8*), as well as another (*ELI3*) from parsley (*Petroselinum crispum*) were described (Kiedrowski et al., 1992), but with no biochemical functions identified at that time. At about the same time, a celery (*Apium graveolens* var. *rapaceum*) homologue to ELI3 (~80/70% similarity/identity) was isolated and reported as a mannitol dehydrogenase, even though K_m values for mannitol were extraordinarily high (72 mM) (Stoop and Pharr, 1992; Stoop et al., 1995; Williamson et al., 1995). More recent contributions by Somssich et al. (1996) and Logemann et al. (1997) later described the *A. thaliana* ELI3-2 (AtCAD8) and the parsley ELI3 as presumed aromatic alcohol oxidoreductases/cinnamyl alcohol dehydrogenases, based on kinetic parameters obtained in vivo with K_m's in the micromolar range. To date, the current annotation of AtCAD2, 3, 6–9 as probable mannitol dehydrogenases lack any form of biochemical/physiological verification, in contrast to the study in celery. Thus, such annotations should be discontinued in the absence of reliable biochemical or other confirmation.

Similar confusion about putative gene function holds as regards physiological/biochemical functions of the recently annotated 12-membered putative rice (*Oryza sativa*) CAD gene family (Tobias and Chow, 2005); in that study, however, none of these had any unambiguously established physiological/biochemical functions. Indeed, nor were any attempts made to correlate known biochemical data (Kim et al., 2004) to level of gene homology in the rice "CAD" family. Since then, a rice CAD (so-called gold hull and internode 2 GH2 gene) has been identified as partially involved in lignin deposition (Zhang et al., 2006); this enzyme has ~84% similarity and ~72% identity to AtCAD4 and AtCAD5. Upon inspection, this rice CAD mutant results from a single Gly185Asp mutation, a region within the Rossman fold, and which is thus three amino acid residues away from the well-known NADPH-binding domain (Youn et al., 2006).

Further indication that AtCAD4 and AtCAD5 were substantially involved in monolignol and (lignified) vascular apparatus formation was recently reported using an *Arabidopsis* CAD (AtCAD4/5) double mutant (Sibout et al., 2005). At maturity, this mutant afforded stem sections which gave estimated "Klason lignin" contents apparently reduced by *circa* 40% relative to wild type (WT). Significantly, the amounts of thioacidolysis releasable monomers **11**–**13** (Fig. 2) from the lignin macromolecule (i.e. of *p*-coumaryl (**6**)/coniferyl (**8**)/sinapyl (**10**) alcohol origin), presumably formed through cleavage of the predominant 8-*O*-4′ linkages in lignin, were extensively reduced (~94%). Thus, whether these plant lines actually contained lignin to any extent is debatable (Jourdes et al. 2007, accompanying manuscript).

From these studies, Sibout et al. (2005) also concluded that there was no compelling evidence for a *substrate-specific* sinapyl aldehyde (**5**)/sinapyl alcohol (**10**) dehydrogenase (SAD) for syringyl (sinapyl alcohol (**10**)-derived) lignin formation as claimed earlier (Li et al., 2001). This was, therefore, in agreement with previous deductions (Anterola and Lewis, 2002; Kim et al., 2004); all known CAD's (as well as the putative SAD) display fairly broad and *not* specific substrate versatilities. Nor was there any evidence obtained for a specific SAD in rice (Zhang et al., 2006).

In the double knockout mutant of AtCAD5 and AtCAD4, the amounts of coniferyl (**3**) and sinapyl (**5**) aldehydes reportedly increased some 55 and 27 fold, respectively, relative to WT (Sibout et al., 2005). However, taken together their levels only accounted for *circa* 0.12% of the overall extractive-free cell-wall residue (CWR). Such amounts are of interest given the various reports (Chabannes et al., 2001; Jones et al., 2001; Morreel et al., 2004; Ralph et al., 2001) that lignins can *efficiently* incorporate either abnormal or non-monolignol entities into *core* (primary) lignin struc-

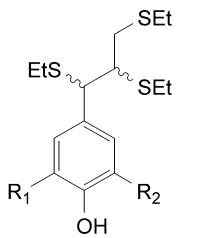

Fig. 2. Typical lignin derived monomeric fragments released from cleavage of presumed 8-*O*-4′ linked substructures in the lignin macromolecule by thioacidolysis. H (**11**), G (**12**) and S (**13**) type lignin unit (or monomer).

tures should monolignol **6**, **8** and **10** supply be reduced in some manner, i.e. via a so-called "combinatorial" biochemistry (Ralph et al., 2004). This particular viewpoint continues to be either reinterpreted upon further analysis (Anterola and Lewis, 2002; Davin and Lewis, 2005), and/or disproven (Anterola and Lewis, 2002; Laskar et al., 2006; Patten et al., 2005), when various plant systems were comprehensively examined. Perhaps, more importantly, the corresponding mature plants of the AtCAD4/5 double mutant have much weakened vasculature/mechanical integrity in accordance with the reduction in lignin deposition proper (Jourdes et al. 2007, accompanying manuscript). This again underscores the critical requirement for a monolignol-derived lignin, and that lignin primary structure proper is a pre-requisite for vascular tissue robustness/integrity.

Additionally, the formation of very small amounts of monolignol derived cleavable guaiacyl (G)/syringyl (S) monomers in the AtCAD4/5 double mutant potentially implied either an incomplete knockout of original AtCAD4/5 activities, or a more minor involvement of other components of the putative CAD metabolic network, e.g. such as AtCAD2, 3, 7 and 8. In this context, it was shown previously that *p*-coumaryl aldehyde (**1**) served as the best substrate of the phenolic substrates **1**–**5** tested in vitro with these isoforms. Its product, *p*-coumaryl alcohol (**6**), is also generally considered to be involved in early stages of lignification/cell wall formation, whereas the G/S components are laid down at later developmental stages (Fukushima and Terashima, 1991; Terashima and Fukushima, 1988; Terashima et al., 1986; Whiting and Goring, 1982). Thus, using the various promoters obtained for this investigation, this gene expression study enabled us to examine the presumed localization of each CAD isoform, and each CAD homologue, i.e. in terms of determination of their possible involvement in formation of the different components of the vascular apparatus during growth and development. Accounts of this work were initially presented at the Fall Symposium, Donald Danforth Center (Saint Louis, Missouri, November 2003) and at the Phytochemical Society of North American Annual Meeting (Ottawa, Canada, August 2004), as well as in a final report to the National Science Foundation (Lewis and Davin, 2006).

Furthermore, since this general approach is being taken for various gene families, encompassing both monolignol formation and monolignol conversion (e.g. into lignins), as well as for their homologues, a full discussion of the growth/development of *Arabidopsis* is also described in this article.

2. Results and discussion

2.1. Design of AtCAD promoters::GUS constructs and Arabidopsis transformations

Putative promoter regions associated with *AtCAD1–9* were determined on the basis of a TAIR database analysis of the *Arabidopsis* sequences, i.e. of those encompassing upstream regions from each of the *AtCAD1–9* genes to that of the next neighbor. With *AtCAD5*, however, its neighboring gene, tentatively described as aldehyde dehydrogenase 3 (*ALDH3*) (Kirch et al., 2004), was in the reverse orientation relative to *AtCAD5*; *ALDH3* is one of a putative 14-member gene family in *Arabidopsis* whose exact physiological roles are again unknown, but may be stress-associated (Kirch et al., 2005). Nevertheless, its reverse orientation raised the possibility that the corresponding upstream *ALDH3* gene sequence might also serve in a promoter capacity for *AtCAD5*. Accordingly, two putative promoter regions were selected, one with the region upstream of *AtCAD5* to *ALDH3* [named *AtCAD5s* (s for short)], and the other encompassing 0.8 kb of *ALDH3* (named *AtCAD5*). Thus ten promoter constructs (two for *AtCAD5*) were selected to individually transform *Arabidopsis* in order to visualize the corresponding patterns of gene expression.

To achieve better GUS catalytic activity and stability at sample fixation, the binary vector pCAMBIA 1305.2 vector (http://www.cambia.org) harboring the GUS*Plus*™ reporter gene was also utilized (Fig. 3); this particular vector has a glycine-rich protein (GRP) signal peptide for extracellular secretion, thereby enabling rapid visualization of in vivo GUS activities. These vectors, with the corresponding promoter regions, were next used to individually transform *Agrobacterium tumefaciens* (An et al., 1988), and subsequently *Arabidopsis* using the floral dip method (Clough and Bent, 1998) as described below.

Specifically, the deduced promoter regions for *AtCAD4* (1804 bp) and *AtCAD5* (1195 and 1976 bp, respectively) were amplified using sense and antisense primers designed with *Eco*RI/*Nco*I or *Pst*I/*Nco*I restriction enzyme sites (Table 1). The amplified full length *AtCAD4*, *AtCAD5s* and *AtCAD5* promoter regions were then individually cloned into a pCR®II-TOPO vector, with the resulting constructs subjected to DNA sequencing for sequence verification. Promoter specific internal primers (Table 2) were used when needed to obtain complete sequence confirmation. In a comparable manner, the promoter regions for *AtCAD1–3* and *6–9* were individually obtained (i.e. 397, 2051, 2032, 585, 600, 1721 and 1637 bp, respectively, Table 1). For *AtCAD2* and *3*, only an ~2 kb 5′ upstream region was used due to the very large untranslated regions between the protein coding sequences, i.e. 3251 and 4918 bp, respectively.

2.2. GUS histochemical localization: general protocols

GUS staining of *Arabidopsis* tissue was carried out using T_2 plants at weekly intervals from 3 days after germination to 9 weeks, i.e. until maturation/senescence. To confirm that the various putatively transformed plant lines contained the correct promoter construct, a rosette leaf from each *AtCAD*::*GUS* transformed *Arabidopsis* line was sampled 21 days after germination, with genomic DNA

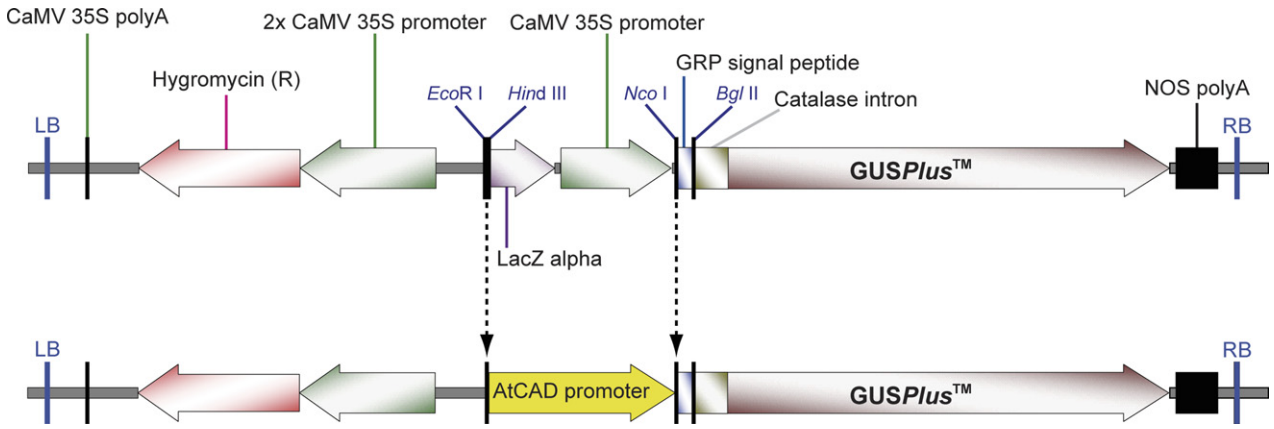

Fig. 3. Schematic diagram of *AtCAD* promoter construction in pCAMBIA1305.2 binary vector. Gene expression of the glycine-rich protein (GRP) signal peptide and the GUS*Plus*™ reporter gene were regulated by each *AtCAD* promoter region in place of the LacZ alpha and CaMV 35S promoter in the pCAMBIA vector. For selection, the pCAMBIA1305.2 vector contains the hygromycin resistance gene downstream of the strong (2×) CaMV 35S promoter.

Table 1
Gene specific primer sequences used for amplification of 5′-flanking promoter region

Construct	Locus	Promoter size (bp)	Restriction site	Forward primer	Reverse primer
AtCAD1::*GUS*	At1g72680	397	*Eco*RI/*Nco*I	5′-GAATTCCGCCATCGATG GTTTTTGTC-3′	5′-CCATGGGCACTCGTTTT CCACACTCTC-3′
AtCAD2::*GUS*	At2g21730	2051	*Eco*RI/*Nco*I	5′-GAATTCCCCTTCTTCATA ATCATATGG-3′	5′-CCATGGTTCGTCGTTG GCCGCCCAACC-3′
AtCAD3::*GUS*	At2g21890	2032	*Eco*RI/*Nco*I	5′-GAATTCCCCTTTTTTGGAA GTACTAGC-3′	5′-CCATGGGTTGGCCGCCC AACCAAATGC-3′
AtCAD4::*GUS*	At3g19450	1804	*Eco*RI/*Nco*I	5′-GAATTCTCTAGAGTCGAA ACTTGTGAC-3′	5′-CCATGGTAAAGCCTTCTTTT CTCCTGC-3′
AtCAD5s::*GUS*	At4g34230	1195	*Eco*RI/*Nco*I	5′-GAATTCGAAGCTTCGTCA TGACTTGGG-3′	5′-CCATGGGCCTGTTGTTTTCC TCTCTGC-3′
AtCAD5::*GUS*	At4g34230	1976	*Pst*I/*Nco*I	5′-CTGCAGTGAGAAATTCTCC ACTCGTAGC-3′	5′-CCATGGGCAGCCCAGCCT GTTGTTTTCC-3′
AtCAD6::*GUS*	At4g37970	585	*Eco*RI/*Nco*I	5′-GAATTCGGAAGGTCCTTCC GGAGTTTG-3′	5′-CCATGGTACGCTCTGCT CTTTCTCTCC-3′
AtCAD7::*GUS*	At4g37980	600	*Eco*RI/*Nco*I	5′-GAATTCTAATACATTGG CTGCTACTCG-3′	5′-CCATGGCAATCCAAACGCC TCCTTCTC-3′
AtCAD8::*GUS*	At4g37990	1721	*Eco*RI/*Nco*I	5′-GAATTCCCAACTCCTTAA CTAGAAAGC-3′	5′-CCATGGTAATCCGAACG CCTCTTTCTG-3′
AtCAD9::*GUS*	At4g39330	1637	*Hin*dIII/*Nco*I	5′-AAGCTTGAGGCGAAAACA GAGTAGGTG-3′	5′-CCATGGAAAGACTTTGTTC GGATGCTC-3′

* Restriction enzyme recognition site on each primer is underlined.

Table 2
Promoter specific internal primer sequences used for promoter sequence analysis

Construct		Internal forward primer	Internal reverse primer
AtCAD2::*GUS*		5′-GTCTGAAATGAGTAGTGGCTCGTC-3′	5′-ACATGCAGAAATCCTCATTGGTAG-3′
AtCAD3::*GUS*	Primer-1	5′-CTCTTTTCCCACCTCCTCCTTTGG-3′	5′-CATGCAGAAATCCTCATTGG-3′
	Primer-2	5′-GAAAACTGGGTTTTGAGTCCCACT-3′	
AtCAD4::*GUS*	Primer-1	5′-CAGTACCTAACCGAACAAAGACTG-3′	
	Primer-2	5′-TTCGTAATAGAGCAACTCTTTCGC-3′	
AtCAD5::*GUS*		5′-CATTGGCCCCATTTACAGCCACAAGTC-3′	5′-GGACAAAGAGTGTGTGAATGGCTTCAC-3′
AtCAD8::*GUS*	Primer-1	5′-GAATATGTTACGTGGACGGAACTG-3′	5′-GAACGTGGACCTTGTGCAACCAC-3′
	Primer-2		5′-GTCACGGAACATGAGCAGTCGATC-3′
AtCAD9::*GUS*	Primer-1	5′-GAGTAAGAACCGGGTCGGAAATAC-3′	
	Primer-2	5′-GTGATGTGTAACGAGGATGAAGAC-3′	

individually isolated, PCR amplified and sequenced, using vector-specific and promoter-specific internal primers (see Experimental). For staining visualization of all tissues and organs (except the stems), and in order to minimize β-glucuronidase product diffusion using X-Gluc (1 mM) as substrate, a solution of 5 mM $K_3Fe(CN)_6/K_4Fe(CN)_6$,

was added to the staining solution. By contrast, in order to obtain high quality stem cross-sections (~0.2-mm thick) for staining, an additional fixation step [0.5% (v/v) formaldehyde for 1 min] was utilized before sectioning (Sibout et al., 2003), followed by exposure of the resulting cross-sections to an 0.5 mM X-Gluc staining solution for 20–60 min. The results obtained for each developmental stage are described below.

2.3. Aerial tissue gene expression during cotyledon and hypocotyl emergence

By 3 days post-germination, two cotyledons and the primary root (discussed separately later) of *Arabidopsis* had emerged from the seed, with the hypocotyl gradually elongating along the primary axis (Figs. 4.1–4.10). At the same time, the primary root hairs and lateral roots had begun to form as well. At this stage, the aerial vascular apparatus (i.e. tracheary elements involved in water conduction) had developed in both the radicle and the cotyledons, with the xylem of the hypocotyl and cotyledon vein tissues apparently lignified (Dharmawardhana et al., 1992).

In terms of gene expression, both *AtCAD4*::*GUS* and *AtCAD5*::*GUS* (1956 bp) displayed very similar patterns of GUS expression (Figs. 4.1 and 4.2). [By contrast, no significant level of expression was observed using the shorter *AtCAD5s*::*GUS* promoter (Fig. 4.3) and indeed essentially no expression was noted with this (short) promoter at all stages of growth/development.] That is, both *AtCAD4*/*5* were strongly expressed in different parts of the developing vascular apparatus, i.e. in the primary and secondary veins of cotyledons in harmony with a role in lignin formation.

For the isoforms displaying much weaker CAD activity in vitro (Kim et al., 2004), no GUS expression was observed for *AtCAD2*::*GUS* (Fig. 4.4), whereas *AtCAD3*::*GUS* was only detected in the apical meristematic regions (Fig. 4.5). While the true biological function/physiological significance of AtCAD3 is unknown, these data apparently do provide an identification of the individual tissues where its gene expression occurs. This is, therefore, a future target at the cellular level in order to probe function, e.g. using either WT and/or various knockout lines, and/or metabolomic analysis of individual cell types as needed.

With *AtCAD7*::*GUS* and *AtCAD8*::*GUS*, however, strong expression was also observed in the vascular apparatus in a manner similar to that of *AtCAD4*/*5*, i.e. in the cotyledon veins and hypocotyl (Figs. 4.6 and 4.7). Moreover, although AtCAD1, 6 and 9 had no detectable CAD activities in vitro, their expression, nevertheless, was also observed in the vasculature, i.e. all were mainly localized to the cotyledon veins (Figs. 4.8–4.10), whereas with *AtCAD9* it was expressed throughout the hypocotyl. Interestingly, GUS staining was additionally observed at the base of the hypocotyl for *AtCAD1*::*GUS* and *AtCAD6*::*GUS*, respectively, the significance of which is unknown.

2.4. Aerial tissue gene expression during rosette and cauline leaf emergence/maturation

2.4.1. First and second rosette leaf development

By ~7 days post-germination, the lignified cotyledons are more mature, the hypocotyl contains well-developed lignified vascular tissues, and the primary roots are continuously elongating (Dharmawardhana et al., 1992). A pair of rosette leaves had now emerged from the apical meristem, as well as lateral roots and root hairs on the primary roots. Unlike the cotyledons, which had only primary and secondary veins, the rosette leaf vascular apparatus had differentiated up to quaternary venation. This section, however, again addresses only the aerial tissues, as the root tissues are described separately later.

By ~14 days, the cotyledons and first rosette leaves had matured further. At this stage, while the second rosette leaves had developed and fully expanded, a set of third rosette leaves had just emerged from the apical meristem. The second and third set of rosette leaves now had more complex (lignified) venation patterns than the first leaves, with the numbers and distribution of trichomes and hydathodes having notably increased (Dharmawardhana et al., 1992).

Additionally, differentiation of the primary veins in the rosette leaves had initiated from the procambium consisting of protoxylem and metaxylem towards the leaf apex. After maturation, the secondary veins had differentiated from the apex of the primary vein and had developed basipetally, after which tertiary vein formation began to occur basipetally from the secondary veins (see Fig. 5.1), and subsequently the quaternary veins (Turner and Sieburth, 2003).

At 7–14 days, the expression patterns of both *AtCAD4*::*GUS* and *AtCAD5*::*GUS* were very similar; for example, GUS expression was observed in the veins of the cotyledons, hypocotyl, apical meristematic region, and in the vascular apparatus of the first rosette leaves, including the hydathodes and trichomes (see Figs. 4.11 and 4.12 at 7 days). Hydathodes, formed at the edge of the rosette leaves, are in close proximity to the ends of the vascular (vein) system (see Fig. 5.1). They are exit points of xylem vessels consisting of a cluster of tracheary elements involved in water conduction (Candela et al., 1999), as well as guttation, i.e. where sap containing metabolites, proteins, and ions is secreted into the atmosphere connected with epithem (stomata) (Pilot et al., 2004). While lignification has been previously reported associated with hydathodes in response to bacterial pathogen attack (Gay and Tuzun, 2000), these data are also suggestive of constitutive expression/lignin deposition.

Additionally, in *Arabidopsis*, the trichomes are unicellular structures that are either branched singularly, or have three to five branches (see Fig. 5.1) with a three-dimensional architecture. These tubular cells are derived from the epidermis, and can extend/branch during cell division (Larkin et al., 1996; Mathur and Chua, 2000; Schwab

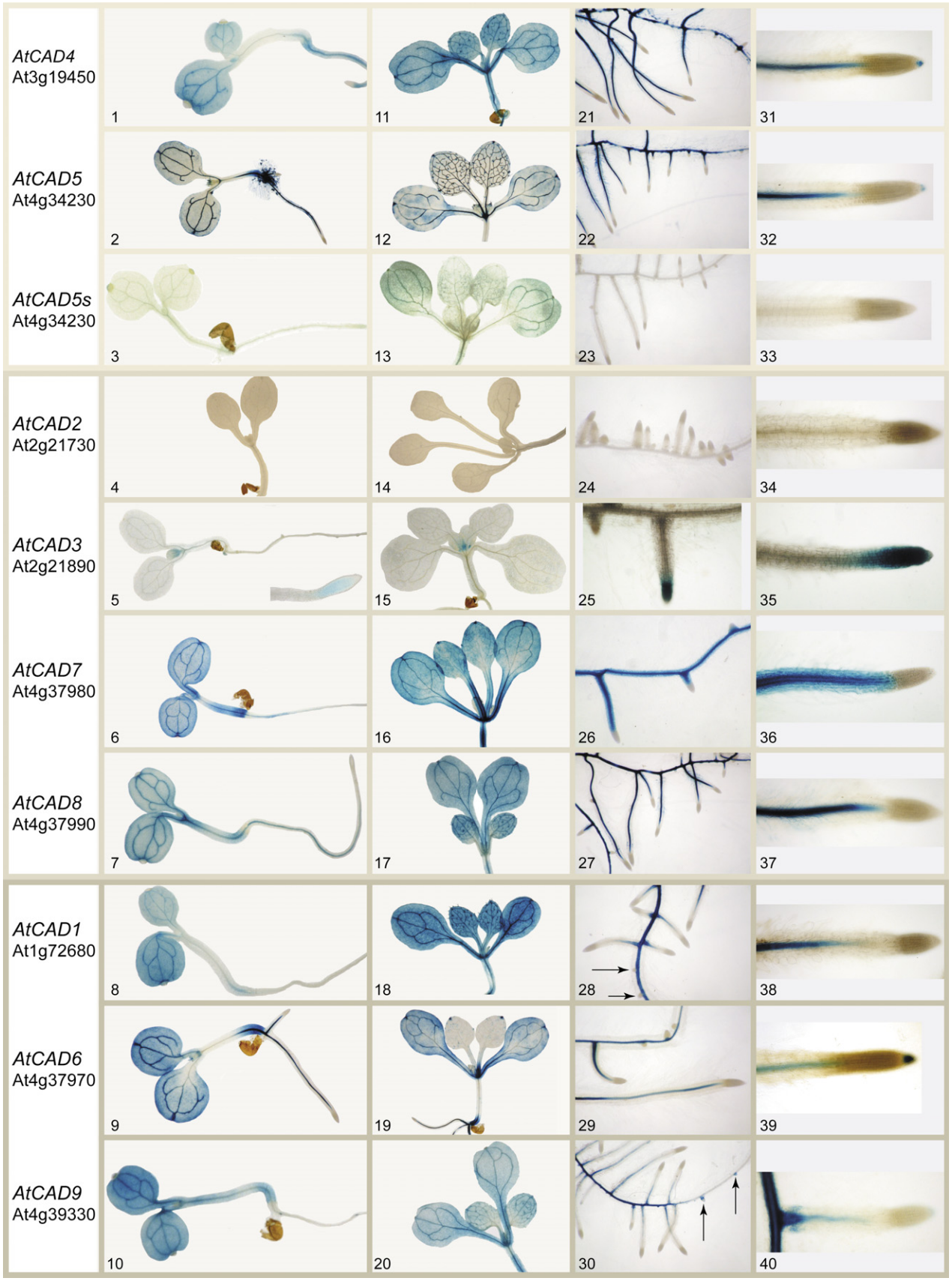

Fig. 4. Histochemical localization of GUS expression of *AtCAD1–9* genes at early stages of *Arabidopsis* development: 3 day old seedlings (1–10) and 7 day old seedlings (11–40). Arrows in 28 and 30 indicate lateral root initiation sites.

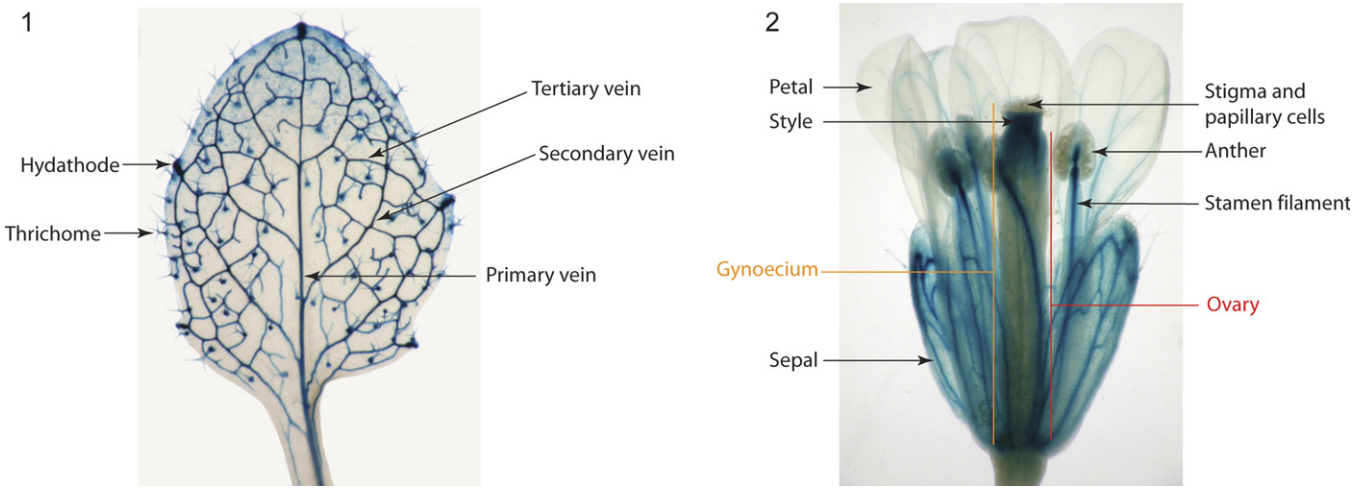

Fig. 5. Anatomy of a rosette leaf (from the second pair) and floral tissues.

et al., 2000). Trichomes have several proposed physiological functions. These include: prevention of water evaporation through formation of a boundary layer on the leaf surface; formation of highly reflective hairs covered with cuticle/waxy material to protect against excessive sunlight (Esau, 1967); suspected detoxification functions for heavy metals, as well as an ability to respond to several other environmental stress conditions, such as salt stress and encroachment by pathogens, e.g. fungi, pests or insects (Gutiérrez-Alcalá et al., 2000).

The major components of mature trichomes are their thick cell walls, which have been described as mainly consisting of cellulose and lignin. In particular, the base of trichomes has been reported as having lignified cells to support the overall structure (Esau, 1967). The expression data for AtCAD4/5 are thus consistent with either a presumed role in lignification or in plant defense. [As noted for the earlier stages of development, however, *AtCAD5s*::*GUS* has apparently only a faint level of GUS expression in the veins of the cotyledons and the hypocotyl (Fig. 4.13). Thus, it is again interesting to note that the upstream *ALDH3* gene sequence serves in a promoter capacity for *AtCAD5*. Since at later stages of development no staining was observed in the plants transformed with *AtCAD5s*::*GUS*, only data obtained with the longer *AtCAD5* promoter is shown].

With *AtCAD2*::*GUS*, there was again no detectable GUS expression in any aerial tissues (i.e. the cotyledons, hypocotyl, and first rosette leaves) (Fig. 4.14), whereas for *AtCAD3*::*GUS*, expression was again specifically restricted to the apical meristematic region (Fig. 4.15).

By contrast, the *AtCAD7* and *AtCAD8* genes were apparently strongly expressed in the vascular apparatus, i.e. of the mature cotyledons, the hypocotyl and the first rosette leaves (Figs. 4.16 and 4.17), in a manner somewhat similar to that of *AtCAD4/5*.

By days 7–14, the GUS expression patterns of *AtCAD1*::*GUS* and *AtCAD9*::*GUS* were also evident throughout the entire vascular apparatus of the cotyledons and first rosette leaves (Figs. 4.18 and 4.20) in a similar pattern to that of *AtCAD4*::*GUS*, *AtCAD5*::*GUS*, *AtCAD7*::*GUS* and *AtCAD8*::*GUS*. By contrast, while *AtCAD6*::*GUS* also had detectable GUS expression in the cotyledon veins and apical meristematic region, there was no detectable expression in the vascular tissues of the first rosette leaves, except for the hydathodes (Fig. 4.19).

2.4.2. Rosette and cauline leaf emergence to maturation

At the 3 week developmental stage, most rosette leaves had developed and were fully expanded. The bolting stem had also emerged where it continues to elongate over the next few weeks. By 4 weeks growth, cauline leaves had developed on the "bolting" stem from the axillary meristem of the branches with formation of a complex venation pattern (data not shown).

The expression patterns of both *AtCAD4*::*GUS* and *AtCAD5*::*GUS* were again very similar in the rosette and cauline leaf tissues. That is, expression in both cases was observed during growth/development from 2 to 7 weeks in the veins, hydathodes, and at the base of trichomes of the vascular apparatus (see Figs. 6.1, 6.2, 6.6 and 6.7 for examples) as before.

For the *AtCAD2*::*GUS*, *AtCAD3*::*GUS*, *AtCAD7*::*GUS* and *AtCAD8*::*GUS* transformants, the patterns of GUS gene expression in the rosette and cauline leaf tissues were also quite instructive. For *AtCAD2*::*GUS*, no expression was again observed in any of the developing leaf tissues from 2 to 5 weeks (Figs. 6.10 and 6.11), with only faint expression being noted sporadically in lesions of senescing (withering) leaf tissues (7–9 weeks) perhaps indicative of a defense and/or senescence-related role (data not shown). Additionally, only very weak GUS expression for *AtCAD3*::*GUS* was noted at the base of the trichomes and in the veins of rosette leaves from 7 to 8 weeks (Figs. 6.14 and 6.15), as well as in the tips of senescing leaf tissue where withering was occurring, i.e. again perhaps indicative of a defense and/or senescence function (data not

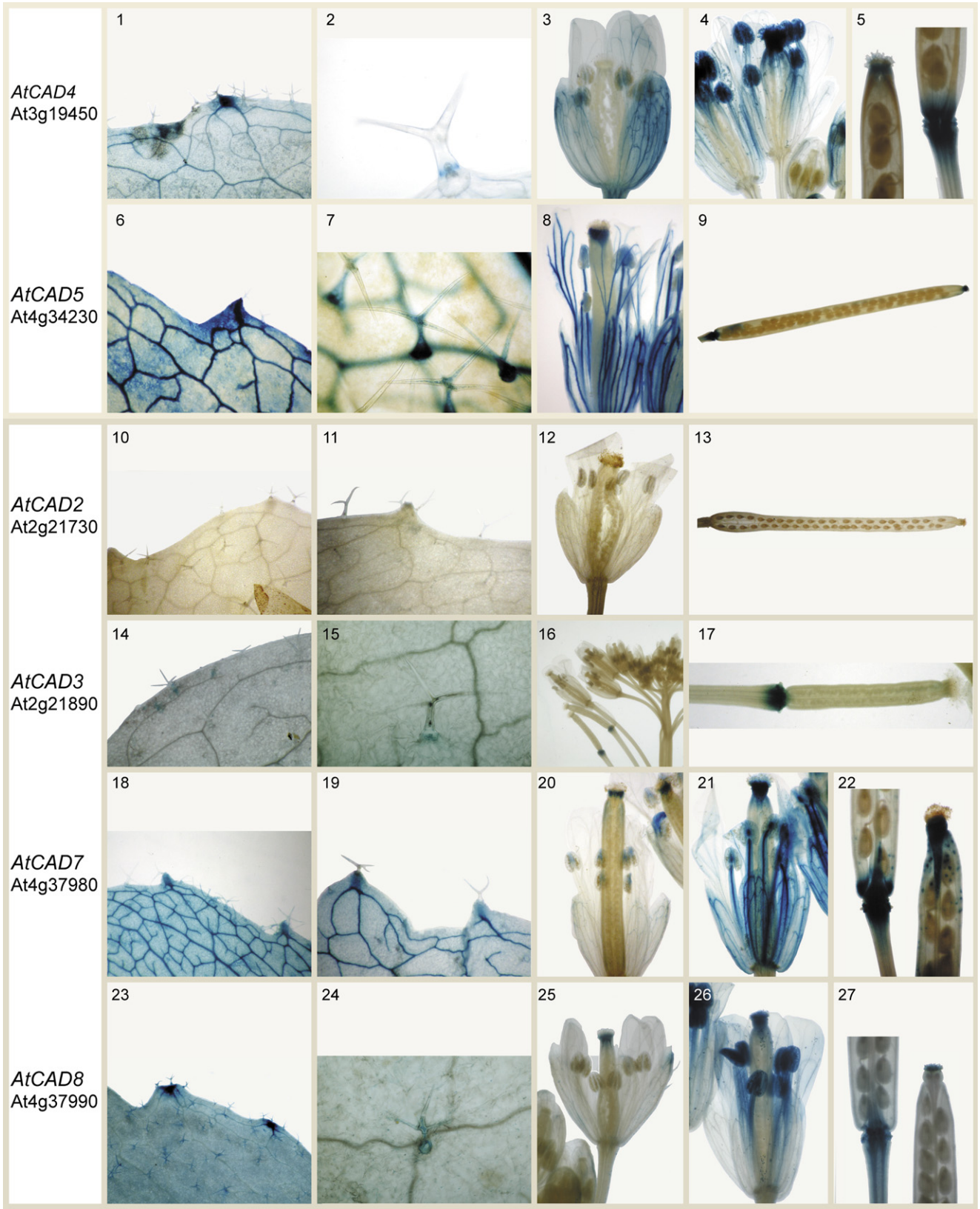

Fig. 6. Histochemical localization of GUS expression of *AtCAD2–5* and *7–8* genes in 3–8 week old *Arabidopsis* leaf tissues and floral organs.

shown). Most importantly, these data tend to indicate that neither AtCAD2 nor 3 had any significant roles in the early stages of lignin deposition.

By contrast, *AtCAD7*::*GUS* was very strongly expressed in the vein and hydathode vasculature, and more weakly in the trichomes from weeks 2 to 7 (Figs. 6.18 and 6.19). By 9

weeks maturation, however, expression was now essentially absent except in regions surrounding the hydathodes of senescing tissues (data not shown). The GUS expression pattern of *AtCAD8*::*GUS* was also quite distinct, being mainly noted in the hydathodes and trichomes of rosette and cauline leaves from 2 to 7 weeks (Figs. 6.23 and 6.24).

Additionally, the *AtCAD1*::*GUS*, *AtCAD6*::*GUS* and *AtCAD9*::*GUS* *Arabidopsis* transformants showed very diverse patterns of gene expression. For *AtCAD1*::*GUS*, the major region of expression from weeks 2 to 8 was in the hydathodes and at the base of the trichomes (Fig. 7.2). Expression in the veins was also observed where the leaf tissue was damaged (Fig. 7.1). Strong expression levels were noted for *AtCAD6*::*GUS* in the vein vasculature and the hydathodes (Figs. 7.6 and 7.7), this gradually reducing in intensity by 7 weeks (data not shown). By contrast, while *AtCAD9*::*GUS* was essentially specifically expressed throughout the vasculature apparatus up to 2 weeks, it was only faintly detected in the hydathodes and trichomes of the rosette and cauline leaves at the later stages (Figs. 7.11 and 7.12). Thus, once again, these sites of gene expression reveal the cellular targets where other technologies, such as knockouts/single cell dissection and metabolite analysis, etc., need to be carried out to attempt to rigorously identify/establish biochemical function(s).

2.5. Gene expression during primary and lateral root elongation and maturation

The *Arabidopsis* root tissue can conveniently be classified into the three regions of differentiation, elongation, and meristem. Of these, lignification apparently occurs only in the differentiation/elongation regions containing the vascular cylinder consisting of xylem and phloem tissues (Esau, 1967; Scheres et al., 2002). On the other hand, there is no known lignification occurring in either the root cap or the root tip meristem. The root cap, composed of living parenchyma cells containing starch, is derived from root epidermal cells, and protects the root apical meristem, as well as in aiding root penetration of the soil in conjunction with perception of gravity (Matsuyama et al., 1999). It is also mechanically strong and is rapidly regenerated when removed through damage. In addition, the root cap has a group of secretory vesicles for secretion

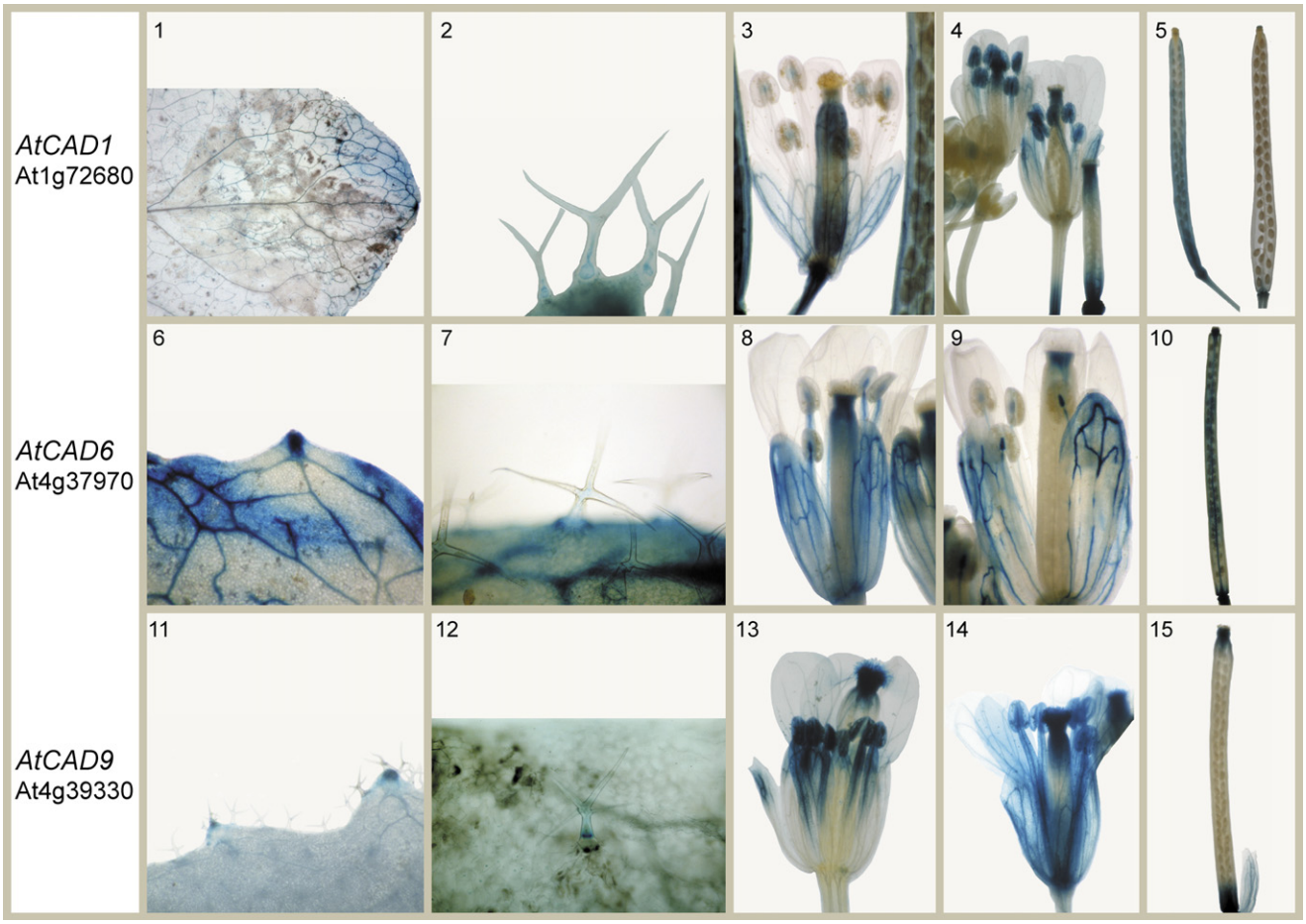

Fig. 7. Histochemical localization of GUS expression of *AtCAD1*, *6* and *9* genes in 3–8 week old *Arabidopsis* leaf tissues and floral organs.

of various metabolites, i.e. proteins, into the mucilage layer that covers the root apex and assists in sloughing of root cap cells (Esau, 1967; Matsuyama et al., 1999). The root meristem, by contrast, is primarily involved in the constant progression of cell division (de Obeso et al., 2003).

In terms of GUS expression, by 3–14 days growth post-germination, both *AtCAD4*::*GUS* and *AtCAD5*::*GUS* were strongly expressed in the primary/lateral root (vascular) tissues (Figs. 4.1, 4.21, 4.31, 4.2, 4.22 and 4.32). Strong GUS expression for both was also noted in the initiation sites for lateral roots developed from the primary root. Interestingly, GUS expression was noted as well for *AtCAD4* and *AtCAD5* in the root caps (Figs. 4.31 and 4.32). Since lignification has never been demonstrated to occur in root caps (Sasaki et al., 1996), this may indicate an alternate role in, for example, plant defense. Additionally, in the elongating primary and lateral roots, there was no GUS expression in the root tips as expected, i.e. where the non-lignifying meristematic region is located. By contrast, in the *AtCAD5s*::*GUS*, no GUS expression in the primary/lateral root tissues including root tips and caps was again observed (Figs. 4.3, 4.23 and 4.33).

For *AtCAD2*::*GUS*, there was no detectable GUS expression in any of the root tissues throughout the entire life span of the organism (Figs. 4.24 and 4.34), whereas for *AtCAD3*::*GUS*, a strong pattern of expression was restricted to the root tips containing the unlignified meristematic region (Figs. 4.5, 4.25 and 4.35). This highlights the need to target the meristem in order to attempt to determine the biochemical function of this gene, and whether it has any role or not in any form of phenylpropanoid metabolism, excluding lignification. For *AtCAD7*::*GUS* and *AtCAD8*::*GUS*, expression followed a similar pattern to that of *AtCAD4*::*GUS* and *AtCAD5*::*GUS*, i.e. in the differentiation and elongation zones of both primary and lateral roots (Figs. 4.6, 4.26, 4.36, 4.7, 4.27 and 4.37). Interestingly, in this case, there was no detectable expression in the root caps in contrast to *AtCAD4*::*GUS* and *AtCAD5*::*GUS*. At 7–8 weeks, faint GUS activity was also observed in mature roots even in the lateral root initiation sites (data not shown).

For *AtCAD1*::*GUS*, initially there was no GUS expression in the primary root at 3 days (Fig. 4.8), while strong expression was observed in the primary root vasculature after 7 days growth (Fig. 4.28). Gene expression was also not evident in the lateral root initiation sites of the primary root or elongating lateral roots (Fig. 4.28, shown by an arrow). As maturation of lateral root development progressed, however, GUS expression became restricted to the vascular apparatus in the elongating regions, but not in the root tips (Figs. 4.28 and 4.38). For *AtCAD9*::*GUS*, there was also no GUS activity noted in the primary root tissues at 3 days (Fig. 4.10); however, as for AtCAD1, there was strong expression noted in the primary root as well as in the lateral root initiation sites by 7 days (Fig. 4.30, shown by arrows), but not in the meristematic root tips or root caps (Figs. 4.30 and 4.40). As lateral root maturation progressed, the GUS expression pattern was initiated from the primary roots along the extending direction of the lateral roots (Figs. 4.30 and 4.40). GUS expression patterns for *AtCAD6*::*GUS* were also similar to *AtCAD4*::*GUS* and *AtCAD5*::*GUS*, i.e. in the primary and lateral roots, as well as in the unlignified root caps (Figs. 4.9, 4.29 and 4.39).

2.6. Gene expression during stem bolting and maturation

The vascular bundles in the ''bolting stem'' consist of xylem and phloem tissues and are involved in water conduction and transport of organic assimilates, respectively (Dharmawardhana et al., 1992). These tissues consist of protoxylem and metaxylem and are differentiated from the procambium located between metaxylem and metaphloem (Esau, 1967; Parker et al., 2003; Patten et al., 2005).

In the *Arabidopsis* stem, the vascular bundles are formed in a ring and are separated by differentiation of interfascicular regions through maturation (Esau, 1967; Patten et al., 2005; Zhong et al., 1997). The latter are comprised of interfascicular cambium involved in development of additional vascular tissues and interfascicular fibers (*if*) which have a mechanical support function for the acropetal growth of the hypocotyl and inflorescence stem (Ehlting et al., 2005; Little et al., 2002; Patten et al., 2005; Zhong et al., 1997). The *Arabidopsis* vascular bundles are arranged as the collateral type, where the xylem develops inside of the phloem. In addition, the vascular bundles contain vascular cambium derived from procambium between xylem and phloem for possible future growth, i.e. for development of secondary vascular tissues (Little et al., 2002; Patten et al., 2005; Zhong et al., 1997).

In the inflorescence stems of *Arabidopsis*, lignification mainly occurs in the xylem (*xy*) tissues consisting of tracheary elements that contain thickened secondary cell walls and interfascicular fibers (*if*) throughout stem development (see Fig. 8) (Patten et al., 2005; Zhong et al., 2000). Generally, the xylem (*xy*) tissues predominantly consist of guaiacyl (G) lignin only, whereas the interfascicular fibers (*if*) contain both G and syringyl (S) lignins during stem growth and development (Dharmawardhana et al., 1992; Patten et al., 2005; Zhong et al., 2000).

At an early stage of stem development, the differentiation of the vascular bundles with lignified xylem tracheary elements occurs prior to the development of interfascicular fibers (*if*) (Patten et al., 2005). At this stage, the G lignin is deposited preferentially in the xylem (*xy*) cell walls. Later, the S lignin contents in mature stems gradually increase due to formation of interfascicular fibers (*if*) (Ehlting et al., 2005; Patten et al., 2005).

With stem growth and development, intense GUS expression was noted for *AtCAD4*::*GUS* and *AtCAD5*::*GUS* from 4 to 8 weeks in the lignifying tissues in agreement with preliminary studies by Sibout et al. (2003), i.e.

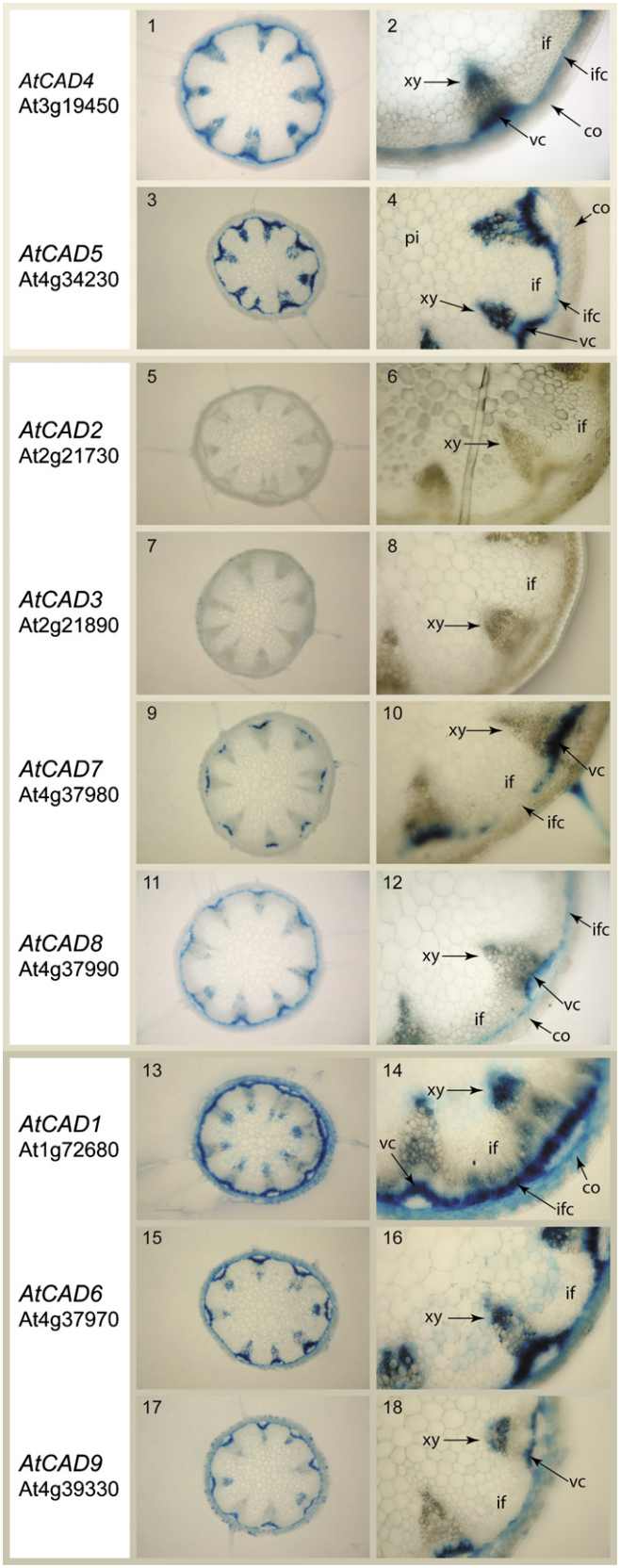

Fig. 8. Histochemical localization of GUS expression of *AtCAD1–9* genes in *Arabidopsis* stem cross-sections. Abbreviations: *xy*, xylem; *vc*, vascular cambium; *ifc*, interfascicular cambium; *if*, interfascicular fibers; *co*, cortex; *pi*, pith. *Note*. Localization was examined at base, middle and top of stems. Due to consistency of data, only basal sections are shown.

in the cells associated with the vascular cambium, interfascicular cambium, and the developing xylem (Figs. 8.1–8.4). However, there was no expression detected in non-lignifying tissues, such as the cortex, the epidermis and the pith. For both genes, there was no indication of expression further into the now lignified interfascicular fibers (*if*) where G and S lignins were deposited. These data are thus consistent with our previous enzyme characterization data (Kim et al., 2004), as well as that of the AtCAD4/5 double mutant (Sibout et al., 2005), i.e. indicating that both AtCAD4 and 5 have dominant roles in monolignol **6**–**10** and lignin formation.

A proteomics analysis of five-week old basal *Arabidopsis* lignifying and non-lignifying stem tissues, however, also indicated that AtCAD5 was potentially present in both tissues at this stage, whereas AtCAD4 was detected only in the lignifying tissues (Cho et al., manuscript in finalization).

With *AtCAD2*::*GUS* and *AtCAD3*::*GUS*, however, there was no detectable level of expression in the stem tissue at any of the 4–8 week growth/development stages examined, again in keeping with both lacking any direct role in macromolecular lignin formation in the stems (Figs. 8.5–8.8). On the other hand, *AtCAD7*::*GUS* expression was readily observable, albeit only in the vascular cambium region from 4 to 8 weeks growth, but not in the interfascicular cambium and fiber regions under the conditions employed (Figs. 8.9 and 8.10). Nor was GUS expression observed in the developing xylem lignifying tissue, the cortex, the epidermis or the pith. GUS-staining of *AtCAD8*::*GUS* was also noted from 4 to 8 weeks, this occurring in the same regions as for *AtCAD4*::*GUS* and *AtCAD5*::*GUS*, i.e. in the vascular cambium and developing xylem tissues (Figs. 8.11 and 8.12). Taken together with the other expression data, this may provisionally suggest a possible (more minor) role for AtCAD7/8 in stem tissue lignification.

Strong levels of GUS expression were also noted for *AtCAD1*::*GUS*, *AtCAD6*::*GUS* and *AtCAD9*::*GUS* from 4 to 8 weeks in the vascular cambium, interfascicular cambium and developing xylem of the stem vascular apparatus (Figs. 8.13–8.18), i.e. as already observed for *AtCAD4*::*GUS*, *AtCAD5*::*GUS* and *AtCAD8*::*GUS*. In addition, GUS activity for *AtCAD1*::*GUS* was also apparently observed in the non-lignifying tissues, such as the cortex region (Figs. 8.13 and 8.14).

2.7. Gene expression during floral apparatus development/maturation

Angiosperms flowers are composed of several reproductive organs (see Fig. 5.2) for development of fruits and seeds through fertilization of the ovules. As a member of the Brassicaceae, *Arabidopsis* produces seed-bearing siliques as its fruits develop from the flowers. The *Arabidopsis* flowers consist of gynoecium, stamen, sepals, and petals, being initially differentiated from the floral meristems,

located in the meristem of the inflorescence stem. After emergence of the flower bud, it is separated from the shoot apex, and four sepals are involved in protection of the flower before opening occurs. At the next stage, the development of petals and stamens begins, and consequently, the flower buds are covered with sepals with the gynoecium primordium differentiation. The latter then develops into an open cylinder form, elongated via differentiation of medial vascular bundles. At this stage, the stamen and petals elongate from the center of the flower bud, followed by development of the placentae, in the gynoecium.

At the next stage, in the gynoecium, the ovule primordium develops from the placentae and differentiation of the lateral vascular bundles is initiated. Differentiation of the carpel walls has thus then begun into the exocarp containing faintly thickened cell walls, as well as in the mesocarp comprised of parenchyma cells and the endocarp with thin cell walls. After formation of the septum in the gynoecium, the stigma and papillary cells develop at the top of the gynoecium, and the short style region is separated from the ovary with growth of the stamen and petals. At this time, the endocarp in the carpel walls differentiates into two layers; the rigid lignified en*b* cell and the unlignified en*a* cell layers. The obvious branching of the medial vascular bundles has occurred at the top of the gynoecium and the ovule development inside the ovary has also been initiated at this stage. The development of the pollen tube, the flower opening, and general pollination occurs then only after the development of stigma and papillary cells has completed with the differentiation of the transmitting tract (Alvarez and Smyth, 2002; Dinneny and Yanofsky, 2005; Ferrándiz et al., 1999; Kuusk et al., 2002; Sessions and Zambryski, 1995).

Lignification of tracheary elements in xylem tissues appears in the late stages of gynoecium development. Following development of procambium, lignification preferentially occurs in the medial vascular bundles. The medial xylem tissues then gradually lignify in both directions, from the base of the gynoecium acropetally and from the developing xylem in the style basipetally, with the two lignified xylem elements ultimately joining around the center of the replum. On the other hand, the lateral xylem tissues are lignified only acropetally from the base of the gynoecium following lignification of the medial bundles. In the style, differentiation of the additional xylem tissues continuously occurs, and the lignified lateral xylem bundles grow upward to the tip of the valves (Alvarez and Smyth, 2002).

For the male reproductive organ system, the *Arabidopsis* stamen is comprised of an anther bearing pollen grains and a filament containing a single vascular strand which is separated from the vascular system of the sporogenous tissue (Esau, 1967). The cell wall of the *Arabidopsis* (and most other flowering plants) anthers is comprised of four layers: epidermis, endothecium, middle layer and tapetum. Among these layers, the endothecial wall plays an important role in anther dehiscence with secondary cell wall thickenings associated with lignification. On the other hand, the cell walls of the stomium and circular cells derived from the epidermis of the anther are not thickened. Lignification has not occurred in these unthickened cell walls, therefore, the stomium and circular cell walls are weaker than lignified endothecial cell walls. Following development of pollen, the anther dehiscence is carried out by shrinkage of different cell wall types, lignified and unlignified walls. Through bursting of the anthers, pollen grains are released from the anthers, and finally, pollination takes place (Dawson et al., 1999).

At the point of anthesis, pollination has occurred and the pollen tubes develop via the transmitting tract growing into the ovules for fertilization. In addition, at this stage, the boundaries of the valves and the replum are also clearly separated. After fertilization, the development of the *Arabidopsis* fruits called "siliques" and seeds begins. In the valve walls, the anticlinal division and longitudinal expansion takes place in the exocarp and mesocarp wall layers, but not in the mesocarp layer located at the edges of the valves adjacent to the replum. Additionally, in the endocarp, the en*b* cells expand longitudinally, while the en*a* cells divide in all directions thus appearing large, round, and swollen. Due to lignin deposition specifically in the en*b* cells, the endocarp wall layers are rigid during silique development and maturation. After xylem lignification, in the medial vascular bundles of the gynoecium, most of the petals and sepals wither; yet, the siliques are continuously extending. Following maturation of siliques, differentiation of the dehiscence region located in the valves and replum margin has occurred (Dinneny and Yanofsky, 2005; Ferrándiz et al., 1999).

The dehiscence region is very important for fruit dehiscence and seed dispersion. As the growing of the valve and septum cells occurs, the outer walls of the exocarp are covered with a thickened cuticle layer, and the en*b* cells develop into schlerenchyma cells, followed by the cells lignifying. With yellowing and drying of the siliques, lignin deposition in the en*b* cells continuously progresses, and degradation of the en*a* cells begins. The pod shattering and seed scattering that then occur subsequently, are performed by a spring-like physical tension mechanism with the lignified en*b* cells. Finally, the siliques are dried-out and opened; thereafter, the seeds are released from the siliques (Dinneny and Yanofsky, 2005; Ferrándiz et al., 1999; Liljegren et al., 2000; Rajani and Sundaresan, 2001).

In terms of development of the floral organs, strong levels of GUS expression were noted for *AtCAD4*::*GUS* and *AtCAD5*::*GUS* from 4 to 8 weeks development. Specifically, in young flowers, this was observed for *AtCAD4*::*GUS* in the anthers where pollen development take place and the sepal veins, but not in the stigmatic region, style, and the petals (Fig. 6.3). In older flowers, however, strong GUS expression was additionally noted in the stigma with the papillary cells (Fig. 6.4). *AtCAD5*::*GUS* displayed a similar pattern of expression, except for the absence of gene expression in the apical stigma which contains the papillary cells (Fig. 6.8). Additionally, the vascular strands in the

petals and sepals were strongly stained as for *AtCAD4*::*GUS*, as well as in the style, the anthers, and the stamen filaments. In the maturing siliques (prior to seed release) of both *AtCAD4*::*GUS* and *AtCAD5*::*GUS* transformants, a strong level of expression was noted, i.e. initially in the stigmatic regions and then in both the abscission and style regions, but not in the seeds themselves (Figs. 6.5 and 6.9). In the internode of the gynoecium (abscission zone), which is known as initiation site of fruit dehiscence, the lignin is longitudinally deposited in the en*b* cells to produce a spring-like physical tension for seed release.

The expression patterns of both *AtCAD2*::*GUS* and *AtCAD3*::*GUS* again differed markedly from that of *AtCAD4*::*GUS* and *AtCAD5*::*GUS*. That is, no GUS expression for *AtCAD2*::*GUS* was observed either in the flowers or in the siliques (Figs. 6.12 and 6.13). With *AtCAD3*::*GUS*, expression occurred only in the abscission zones of newly formed siliques (Figs. 6.16 and 6.17) but not in the mature silique (data not shown). The physiological/biochemical significance of this staining is, however, unknown.

The expression patterns of *AtCAD7*::*GUS* and *AtCAD8*::*GUS* were also quite distinctive. In young flowers, a faint level of GUS expression of both genes was noted in the style and anthers, as well as in the stigmatic regions (Figs. 6.20 and 6.25). As the flowers mature, GUS expression was much more intense and widespread in the style, the anthers containing pollen grains, the stamen filaments, and the vascular tissues of the sepals for *AtCAD7*::*GUS* (Fig. 6.21), as well as in the maturing floral organs of *AtCAD8*::*GUS*, but not in the sepals (Fig. 6.26). Additionally, there were strong levels of expression in the abscission and style regions of the maturing siliques for both, as well as in the stigmatic zone for *AtCAD7*::*GUS* (Figs. 6.22 and 6.27).

Although lacking detectable CAD activities in vivo, the encoding genes of AtCAD1, 6 and 9 were also strongly expressed in the floral organs. Thus, for *AtCAD1*::*GUS*, expression was observed in the style, the vascular strands of the sepals of young flowers (Fig. 7.3), as well as in the anthers with pollen grains in older flowers (Fig. 7.4). GUS activity was also noted in the abscission and stigmatic regions of the developing siliques (Fig. 7.4), in the maturing silique and finally only in the abscission zone of the mature siliques (Fig. 7.5). Expression of *AtCAD6*::*GUS* was also quite pronounced in the entire floral organs from 4 to 6 weeks, although not in either the stigma or petals (Figs. 7.8 and 7.9). Its overall expression patterns in the floral organs were similar to that of *AtCAD5*::*GUS* except for expression in the petal veins. In the siliques, *AtCAD6*::*GUS* was also strongly expressed in the abscission and style regions, as well as in the medial xylem strands (Fig. 7.10). Furthermore, *AtCAD9*::*GUS* was strongly expressed in the stigmatic region containing the papillary cells, style, anthers include pollen, stamen filaments, and sepals of the floral organs (Fig. 7.13). However, at a later stage, GUS expression for *AtCAD9*::*GUS* was evident throughout the entire floral organs (Fig. 7.14) and was quite distinct from that of *AtCAD1*::*GUS*, *AtCAD4*::*GUS* and *AtCAD6*::*GUS*. On the other hand, *AtCAD9*::*GUS* was strongly expressed in the abscission and style regions the siliques including stigmatic regions (Fig. 7.15).

Additionally, laccases (EC 1.10.3.2) are multi-copper enzymes that have often been reported as involved in monolignol polymerization leading to lignins, but for which there is yet no compelling proof (see Lewis et al., 1999). Recently, loss-of-function studies of one *Arabidopsis* laccase isoform, *AtLac14* (At5g48100), had indicated a putative role for laccases in the oxidation of flavonoids in the seed coat (Pourcel et al., 2005). Yet another study, by contrast, also proposed a role in lignification in the seed coat for this laccase isoform (Liang et al., 2006). In this context, promoter–GUS fusions of *AtLac14* (Turlapati et al., manuscript in finalization) indicated that it is indeed expressed in seed coat tissues, but also in other tissues as well. However, by contrast, none of the *bona fide* and/or putative CAD family, including both *AtCAD4*::*GUS* and *AtCAD5*::*GUS*, gave any detectable form of expression in the seed coat tissues under the conditions described. These data suggest that the laccase(s) expressed in the seed coats is (are) involved in physiological processes other than lignification.

2.8. Comparison of GUS expression with microarray gene expression databases

We have also explored the *Arabidopsis* gene expression database at AtGenExpress (http://www.weigelworld.org/resources/microarray/AtGenExpress/) that covers a wide range of developmental stages as well as different organs (Schmid et al., 2005). Expression levels were measured using Affymetrix's GeneChip microarray technology. In brief, *AtCAD5* transcripts were detected in roots, stems, leaves, flowers and siliques, i.e. with the same patterns described above for GUS staining. Interestingly, *AtCAD4* transcript levels were higher in the roots as compared to the other organs and overall lower to those observed for *AtCAD5*. *AtCAD3* transcripts were not observed in any organs analyzed in agreement with GUS staining data. *AtCAD7* transcripts were mainly found in leaves and flowers, whereas *AtCAD8* was mainly only detected in the flowers. *AtCAD1* transcripts levels were highest in stage 8–10 seeds. In contrast to the results observed in this study, *AtCAD6* transcripts were mainly not detected. *AtCAD9* expression levels were the highest overall particularly in the flowers and siliques containing stage 3–5 seeds, the significance of which is unknown.

3. Conclusions

Based on the report by Kim et al. (2004), the nine-membered CAD multigene family and CAD homologues in *Arabidopsis* could be divided into three groups based on

their relative CAD catalytic activities in vitro. To comprehensively delineate the patterns of gene expression of each in vivo, GUS histochemical localization was performed for each potential isoform. Taken together, the results obtained herein (together with studies of Kim et al. (2004) and Sibout et al. (2005)) indicate that AtCAD4 and 5 are mainly involved in the metabolic network for lignin formation in the various forms of the vascular apparatus; provisionally, AtCAD7 and 8 may also be associated with lignification in a more minor way. Interestingly, the promoter region for AtCAD5 had to be extended into the *ALDH3* gene sequence in order for expression to be observed. By contrast, *AtCAD2* and *3* had no GUS expression patterns specific to the vascular system and thus must be considered as involved in other biosynthetic pathways. Additionally, while *AtCAD1*, *6* and *9* displayed similar expression patterns to *AtCAD4* and *5*, their corresponding enzymatic properties in vitro lacked CAD catalytic activity proper in our hands, and thus their true biochemical roles also need to be established.

Most importantly, the gene expression patterns now offer the opportunity to target specific cell types in order to identify true physiological functions of the CAD-like and CAD homologues. This comprehensive analysis also further demonstrates, however, the challenges and opportunities in annotating possible *Arabidopsis* gene functions. This is particularly evident with the (unproven) reclassification of some of these CAD homologues (e.g. AtCAD2, 6–9) as mannitol dehydrogenases, for which there is no biochemical determination supporting such a function in *Arabidopsis*. Determination of gene function is thus a particularly important challenge, as it is currently estimated that only about 12% or so of the *Arabidopsis* genes in 2006, in fact, have a truly known biochemical function (The Multinational Arabidopsis Steering Committee, 2006). Lastly, although not discussed herein, the differential patterns of gene expression under control of these different promoters provides an opportunity in the future to establish what roles the promoter elements have in targeting localization/developmental stages, to specific cells and tissues.

4. Experimental

4.1. Materials

pCR®II-TOPO vector and *Taq* DNA polymerase were purchased from Invitrogen (Carlsbad, CA), whereas pCAMBIA 1305.2 vector was from Cambia (Canberra, Australia). *PfuTurbo*® DNA polymerase was purchased from Stratagene (La Jolla, CA), and the restriction enzymes, *Eco*RI, *Hin*dIII, *Pst*I and *Nco*I, were from New England Biolabs (Beverly, MA). REDExtract-N-AMP Plant PCR Kit was obtained from Sigma (St. Louis, MO) with 5-bromo-4-chloro-3-indolyl-β-D-glucuronide (X-Gluc) from Gold Bio Technology, Inc. (St. Louis, MO). DNeasy® Plant Mini Kit and QIAquick Gel Extraction kits were from Qiagen (Valencia, CA), with the Rapid DNA Ligation Kit purchased from Roche (Indianapolis, IN). Custom oligonucleotide primers for PCR and sequencing were synthesized by Invitrogen.

4.2. Plant material and growth conditions

Wild type *Arabidopsis thaliana* (ecotype Columbia) plants were grown on soil as previously described (Patten et al., 2005), whereas transgenic *Arabidopsis* plants for GUS analysis were grown in growth chambers at 21 °C with a 16 h day/8 h night cycle and a light intensity of 248.5 μmol m^{-2} s^{-1}.

4.3. Isolation of 5′-flanking region of AtCAD1–9 and promoter::GUS vector construction

Rosette leaves of 5-week-old *A. thaliana* (WT) were frozen in liq. N_2, ground to a powder in a mortar, with genomic DNA isolated and purified using a DNeasy® Plant Mini Kit, following the manufacturer's instructions. The 5′-flanking region of each of the 10 *AtCAD* homologues (two for *AtCAD5*) was next individually amplified by PCR using an aliquot of the purified DNA with forward and reverse gene-specific primers designed from the TAIR database (Table 1). The forward primers contained *Eco*RI, *Pst*I or *Hin*dIII sites, whereas the reverse primers had a *Nco*I site (Table 1). The PCR mixture consisted of 0.2 mM each dNTPs, 0.2 μM of forward and reverse primers, 50 ng genomic DNA, 1× Cloned *Pfu* DNA polymerase reaction buffer, and 2.5 U *PfuTurbo*® DNA polymerase, with amplification using the touch-down method described in Kim et al. (2004). After reaction, the PCR products were individually analyzed on an 0.5–1.2% (w/v) agarose gel depending on promoter size, then further purified using the QIAquick gel extraction kit following the manufacturer's instructions, and subsequently cloned into a pCR®II-TOPO vector for sequencing and further pCAMBIA vector construction. For complete sequence confirmation, vector specific primers (M13 forward/reverse) and, if needed, promoter specific internal primers (Table 2) were used. After sequence verification, each promoter region was individually excised from the pCR®II-TOPO vector with the corresponding restriction enzymes as shown in Table 1. In parallel, the pCAMBIA 1305.2 vector was also cleaved with *Eco*RI/*Nco*I (for *AtCAD1* to *8* and *AtCAD5s*), *Pst*I/*Nco*I (for *AtCAD5*) or *Hin*dIII/*Nco*I (for *AtCAD9*) to remove the 35S CaMV promoter. Using the Rapid DNA Ligation Kit, each *AtCAD* promoter region excised from the pCR®II-TOPO vector was individually ligated into the corresponding pCAMBIA 1305.2 vector (Fig. 3). The sequence of each *AtCAD* promoter in the pCAMBIA 1305.2 vector was further confirmed using pCAMBIA vector specific primers (forward: 5′-CCATCTTTGGGACCACTGTCG-3′, reverse: 5′-GCACGATACGCTGATCCTTC-3′) as well as with the corresponding

AtCAD promoter specific primers (Table 1) and, if needed, the promoter specific internal primers (Table 2).

4.4. Arabidopsis transformation and selection

Each construct (*AtCAD1*::*GUS* through *AtCAD9*::*GUS* and *AtCAD5s*::*GUS*) was individually introduced by electroporation (An et al., 1988) into the *Agrobacterium tumefaciens* strain GV3101, with subsequent *Arabidopsis* transformations using the floral dip method (Clough and Bent, 1998). After transformation, plant lines were greenhouse-grown until the siliques were mature and dry. The resulting seeds (T_0) were next harvested, with individual transformant (T_1 plant) lines selected for 2 weeks on MS medium containing hygromycin B (20 mg/*l*, optimized concentration) as selection agent (Hadi et al., 2002) and carbenicillin (100 mg/*l*). Transformants were next transferred to soil and greenhouse-grown until seed (T_1) maturation.

That the plant lines were transgenic was confirmed as follows: a rosette leaf from each 3-week-old transgenic T_2 *Arabidopsis* (*AtCAD1*::*GUS* through *AtCAD9*::*GUS* and *AtCAD5s*::*GUS*) was harvested with the genomic DNA isolated using the REDExtract-N-AMP Plant PCR Kit following the manufacturer's instructions. PCR was next carried out for each using the touch-down method described in Kim et al. (2004) with an aliquot of the extracted genomic DNA, the pCAMBIA vector specific primers and the corresponding *AtCAD* promoter specific primers (Table 1) or promoter specific internal primers, as needed (Table 2). The individual amplified PCR products so obtained were then directly sequenced.

4.5. Histochemical localization of GUS expression

Histochemical GUS analyses were carried out on T_2 plants at 3 days after seeding, and then at weekly intervals from one to nine weeks, i.e. until maturation/senescence. Three to fourteen day old plants were grown on MS medium, whereas plants analyzed at ages from 3 to 9 weeks were grown on soil.

Histochemical staining was as described by Jefferson et al. (1987) and modified by Kim et al. (2006, 2002). Whole plants or detached organs were immediately immersed in GUS staining solution consisting of X-Gluc (1.0 mM), $K_3Fe(CN)_6$ (5 mM), $K_4Fe(CN)_6$ (5 mM), and Triton X-100 (0.5%, v/v) in sodium phosphate buffer (50 mM, pH 7.0). After staining for 3–12 h at 37 °C on an orbital shaker at 30 rpm, plant tissues were bleached several times by washing with aqueous EtOH (3:7, v/v). Stained tissues were analyzed under a dissecting microscope (Wild Photomakroskop M400, Switzerland) with photographs taken by color reversal slide film (Kodak Ektachrome 64T) and scanned.

For stem cross-sectional analyses, sections (~1 cm) were immediately immersed in formaldehyde (0.5%, v/v) for 1 min at room temperature (Sibout et al., 2003). Thick sections (~0.2-mm) were then cut with a double-edge razor blade in sodium phosphate buffer (50 mM, pH 7.0) containing $K_3Fe(CN)_6$ (5 mM), $K_4Fe(CN)_6$ (5 mM), and Triton X-100 (0.5%, v/v). Sections were next transferred into the GUS staining solution (see above) but containing 0.5 mM X-Gluc (instead of 1.0 mM). After 20–60 min incubation at 37°C with shaking, the stained stem cross-sections were bleached with aqueous EtOH (3:7, v/v) and analyzed as described above. Expression patterns were similar between basal, middle and top section of the stem, and only basal sections are shown (Fig. 8).

4.6. Microarray data comparison

Microarray data compiled in the AtGenExpress database (http://www.weigelworld.org/resources/microarray/AtGenExpress/) were analyzed for AtCAD1 and AtCAD3–9, AtCAD2 could not be compared as it is not on the Affimetrix array chip.

Acknowledgements

This research project is supported by the National Science Foundation [MCB-0117260 9 (Arabidopsis 2010) and MCB-041729], the US Department of Energy (DE-FG-0397ER20259), and the G. Thomas and Anita Hargrove Center for Plant Genomic Research. The authors thank Julia Gothard-Szamosfalvi for growing and maintaining plant specimens and Hye-Won Park for assistance with GUS staining.

References

Alvarez, J., Smyth, D.R., 2002. *CRABS CLAW* and *SPATULA* genes regulate growth and pattern formation during gynoecium development in *Arabidopsis thaliana*. Int. J. Plant Sci. 163, 17–41.

An, G., Ebert, P.R., Mitra, A., Ha, S.B., 1988. Binary vectors. In: Gelvin, S.B., Schilperoort, R.A., Verma, D.P.S. (Eds.), Plant Molecular Biology Manual, vol. A3. Kluwer Academic Publishers, Dordrecht, pp. 1–19.

Anterola, A.M., Jeon, J.-H., Davin, L.B., Lewis, N.G., 2002. Transcriptional control of monolignol biosynthesis in *Pinus taeda*: factors affecting monolignol ratios and carbon allocation in phenylpropanoid metabolism. J. Biol. Chem. 277, 18272–18280.

Anterola, A.M., Lewis, N.G., 2002. Trends in lignin modification: a comprehensive analysis of the effects of genetic manipulations/mutations on lignification and vascular integrity. Phytochemistry 61, 221–294.

Candela, H., Martínez-Laborda, A., Micol, J.L., 1999. Venation pattern formation in *Arabidopsis thaliana* vegetative leaves. Dev. Biol. 205, 205–216.

Chabannes, M., Barakate, A., Lapierre, C., Marita, J.M., Ralph, J., Pean, M., Danoun, S., Halpin, C., Grima-Pettenati, J., Boudet, A.M., 2001. Strong decrease in lignin content without significant alteration of plant development is induced by simultaneous down-regulation of cinnamoyl CoA reductase (CCR) and cinnamyl alcohol dehydrogenase (CAD) in tobacco plants. Plant J. 28, 257–270.

Clough, S.J., Bent, A.F., 1998. Floral dip: a simplified method for *Agrobacterium*-mediated transformation of *Arabidopsis thaliana*. Plant J. 16, 735–743.

Costa, M.A., Collins, R.E., Anterola, A.M., Cochrane, F.C., Davin, L.B., Lewis, N.G., 2003. An *in silico* assessment of gene function and organization of the phenylpropanoid pathway metabolic networks in *Arabidopsis thaliana* and limitations thereof. Phytochemistry 64, 1097–1112.

Damiani, I., Morreel, K., Danoun, S., Goeminne, G., Yahiaoui, N., Marque, C., Kopka, J., Messens, E., Goffner, D., Boerjan, W., Boudet, A.M., Rochange, S., 2005. Metabolite profiling reveals a role for atypical cinnamyl alcohol dehydrogenase CAD1 in the synthesis of coniferyl alcohol in tobacco xylem. Plant Mol. Biol. 59, 753–769.

Davin, L.B., Lewis, N.G., 2005. Lignin primary structures and dirigent sites. Curr. Opin. Biotechnol. 16, 407–415.

Dawson, J., Sözen, E., Vizir, I., Van Waeyenberge, S., Wilson, Z.A., Mulligan, B.J., 1999. Characterization and genetic mapping of a mutation (*ms35*) which prevents anther dehiscence in *Arabidopsis thaliana* by affecting secondary wall thickening in the endothecium. New Phytol. 144, 213–222.

de Obeso, M., Caparrós-Ruiz, D., Vignols, F., Puigdomènech, P., Rigau, J., 2003. Characterisation of maize *peroxidases* having differential patterns of mRNA accumulation in relation to lignifying tissues. Gene 309, 23–33.

Dharmawardhana, D.P., Ellis, B.E., Carlson, J.E., 1992. Characterization of vascular lignification in *Arabidopsis thaliana*. Can. J. Bot. 70, 2238–2244.

Dinneny, J.R., Yanofsky, M.F., 2005. Drawing lines and borders: how the dehiscent fruit of *Arabidopsis* is patterned. BioEssays 27, 42–49.

Ehlting, J., Mattheus, N., Aeschliman, D.S., Li, E., Hamberger, B., Cullis, I.F., Zhuang, J., Kaneda, M., Mansfield, S.D., Samuels, L., Ritland, K., Ellis, B.E., Bohlmann, J., Douglas, C.J., 2005. Global transcript profiling of primary stems from *Arabidopsis thaliana* identifies candidate genes for missing links in lignin biosynthesis and transcriptional regulators of fiber differentiation. Plant J. 42, 618–640.

Esau, K., 1967. Plant Anatomy. John Wiley & Sons Inc, New York.

Ferrándiz, C., Pelaz, S., Yanofsky, M.F., 1999. Control of carpel and fruit development in *Arabidopsis*. Annu. Rev. Biochem. 68, 321–354.

Fukushima, K., Terashima, N., 1991. Heterogeneity in formation of lignin. XIV. Formation and structure of lignin in differentiating xylem of *Ginkgo biloba*. Holzforschung 45, 87–94.

Gay, P.A., Tuzun, S., 2000. Involvement of a novel peroxidase isozyme and lignification in hydathodes in resistance to black rot disease in cabbage. Can. J. Bot. 78, 1144–1149.

Gutiérrez-Alcalá, G., Gotor, C., Meyer, A.J., Fricker, M., Vega, J.M., Romero, L.C., 2000. Glutathione biosynthesis in *Arabidopsis* trichome cells. Proc. Natl. Acad. Sci., USA 97, 11108–11113.

Hadi, M.Z., Kemper, E., Wendeler, E., Reiss, B., 2002. Simple and versatile selection of *Arabidopsis* transformants. Plant Cell Rep. 21, 130–135.

Jefferson, R.A., Kavanagh, T.A., Bevan, M.W., 1987. GUS fusions: β-glucuronidase as a sensitive and versatile gene fusion marker in higher plants. EMBO J. 6, 3901–3907.

Jones, L., Ennos, A.R., Turner, S.R., 2001. Cloning and characterization of *irregular xylem4* (*irx4*): a severely lignin-deficient mutant of *Arabidopsis*. Plant J. 26, 205–216.

Kiedrowski, S., Kawalleck, P., Hahlbrock, K., Somssich, I.E., Dangl, J.L., 1992. Rapid activation of a novel plant defense gene is strictly dependent on the *Arabidopsis RPM1* disease resistance locus. EMBO J. 11, 4677–4684.

Kim, K.-W., Franceschi, V.R., Davin, L.B., Lewis, N.G., 2006. β-Glucuronidase as reporter gene: advantages and limitations. In: Salinas, J., Sanchez-Serrano, J.J. (Eds.), second ed., In: Methods in Molecular Biology, vol. 323: *Arabidopsis* Protocols Humana Press, Totowa, NJ, pp. 263–273.

Kim, M.K., Jeon, J.-H., Davin, L.B., Lewis, N.G., 2002. Monolignol radical–radical coupling networks in western red cedar and *Arabidopsis* and their evolutionary implications. Phytochemistry 61, 311–322.

Kim, S.-J., Kim, M.-R., Bedgar, D.L., Moinuddin, S.G.A., Cardenas, C.L., Davin, L.B., Kang, C., Lewis, N.G., 2004. Functional reclassification of the putative cinnamyl alcohol dehydrogenase multigene family in *Arabidopsis*. Proc. Natl. Acad. Sci. USA 101, 1455–1460.

Kirch, H.-H., Bartels, D., Wei, Y., Schnable, P.S., Wood, A.J., 2004. The *ALDH* gene superfamily of *Arabidopsis*. Trends Plant Sci. 9, 371–377.

Kirch, H.-H., Schlingensiepen, S., Kotchoni, S., Sunkar, R., Bartels, D., 2005. Detailed expression analysis of selected genes of the aldehyde dehydrogenase (*ALDH*) gene superfamily in *Arabidopsis thaliana*. Plant Mol. Biol. 57, 315–332.

Knight, M.E., Halpin, C., Schuch, W., 1992. Identification and characterisation of cDNA clones encoding cinnamyl acohol dehydrogenase from tobacco. Plant Mol. Biol. 19, 793–801.

Kuusk, S., Sohlberg, J.J., Long, J.A., Fridborg, I., Sundberg, E., 2002. *STY1* and *STY2* promote the formation of apical tissues during *Arabidopsis* gynoecium development. Development 129, 4707–4717.

Larkin, J.C., Young, N., Prigge, M., Marks, M.D., 1996. The control of trichome spacing and number in *Arabidopsis*. Development 122, 997–1005.

Laskar, D.D., Jourdes, M., Patten, A.M., Helms, G.L., Davin, L.B., Lewis, N.G., 2006. The *Arabidopsis* cinnamoyl CoA reductase *irx4* mutant has a delayed but coherent (normal) program of lignification. Plant J. 48, 674–686.

Lewis, N.G., Davin, L. B., 2006. Final Report on Grant # MCB-0117260 (*Arabidopsis* 2010 Project) to the National Science Foundation, June 30th 2006.

Lewis, N.G., Davin, L.B., Sarkanen, S., 1999. The nature and function of lignins. In: Barton, Sir D.H.R., Nakanishi, K., Meth-Cohn, O. (Eds.), Comprehensive Natural Products Chemistry, vol. 3. Elsevier, Oxford, pp. 617–745.

Li, L., Cheng, X.-F., Leshkevich, J., Umezawa, T., Harding, S.A., Chiang, V.L., 2001. The last step of syringyl monolignol biosynthesis in angiosperms is regulated by a novel gene encoding sinapyl alcohol dehydrogenase. Plant Cell 13, 1567–1585.

Liang, M., Davis, E., Gardner, D., Cai, X., Wu, Y., 2006. Involvement of *AtLAC15* in lignin synthesis in seeds and in root elongation of *Arabidopsis*. Planta 224, 1185–1196.

Liljegren, S.J., Ditta, G.S., Eshed, Y., Savidge, B., Bowman, J.L., Yanofsky, M.F., 2000. *SHATTERPROOF* MADS-box genes control seed dispersal in *Arabidopsis*. Nature 404, 766–770.

Little, C.H.A., MacDonald, J.E., Olsson, O., 2002. Involvement of indole-3-acetic acid in fascicular and interfascicular cambial growth and interfascicular extraxylary fiber differentiation in *Arabidopsis thaliana* inflorescence stems. Int. J. Plant Sci. 163, 519–529.

Logemann, E., Reinold, S., Somssich, I.E., Hahlbrock, K., 1997. A novel type of pathogen defense-related cinnamyl alcohol dehydrogenase. Biol. Chem. 378, 909–913.

Mathur, J., Chua, N.-H., 2000. Microtubule stabilization leads to growth reorientation in *Arabidopsis* trichomes. Plant Cell 12, 465–477.

Matsuyama, T., Satoh, H., Yamada, Y., Hashimoto, T., 1999. A maize glycine-rich protein is synthesized in the lateral root cap and accumulates in the mucilage. Plant Physiol. 120, 665–674.

Morreel, K., Ralph, J., Kim, H., Lu, F., Goeminne, G., Ralph, S., Messens, E., Boerjan, W., 2004. Profiling of oligolignols reveals monolignol coupling conditions in lignifying poplar xylem. Plant Physiol. 136, 3537–3549.

Parker, G., Schofield, R., Sundberg, B., Turner, S., 2003. Isolation of *COV1*, a gene involved in the regulation of vascular patterning in the stem of *Arabidopsis*. Development 130, 2139–2148.

Patten, A.M., Cardenas, C.L., Cochrane, F.C., Laskar, D.D., Bedgar, D.L., Davin, L.B., Lewis, N.G., 2005. Reassessment of effects on lignification and vascular development in the *irx4 Arabidopsis* mutant. Phytochemistry 66, 2091–2107.

Pilot, G., Stransky, H., Bushey, D.F., Pratelli, R., Ludewig, U., Wingate, V.P.M., Frommer, W.B., 2004. Overexpression of *GLUTAMINE DUMPER1* leads to hypersecretion of glutamine from hydathodes of *Arabidopsis* leaves. Plant Cell 16, 1827–1840.

Pourcel, L., Routaboul, J.M., Kerhoas, L., Caboche, M., Lepiniec, L., Debeaujon, I., 2005. *TRANSPARENT TESTA10* encodes a laccase-

like enzyme involved in oxidative polymerization of flavonoids in *Arabidopsis* seed coat. Plant Cell 17, 2966–2980.

Rajani, S., Sundaresan, V., 2001. The *Arabidopsis* myc/bHLH gene *ALCATRAZ* enables cell separation in fruit dehiscence. Curr. Biol. 11, 1914–1922.

Ralph, J., Lapierre, C., Marita, J.M., Kim, H., Lu, F., Hatfield, R.D., Ralph, S., Chapple, C., Franke, R., Hemm, M.R., Van Doorsselaere, J., Sederoff, R.R., O'Malley, D.M., Scott, J.T., MacKay, J.J., Yahiaoui, N., Boudet, A.M., Pean, M., Pilate, G., Jouanin, L., Boerjan, W., 2001. Elucidation of new structures in lignins of CAD- and COMT-deficient plants by NMR. Phytochemistry 57, 993–1003.

Ralph, J., Lundquist, K., Brunow, G., Lu, F., Kim, H., Schatz, P.F., Marita, J.M., Hatfield, R.D., Ralph, S.A., Christensen, J.H., Boerjan, W., 2004. Lignins: natural polymers from oxidative coupling of 4-hydroxyphenylpropanoids. Phytochem. Rev. 3, 29–60.

Sasaki, M., Yamamoto, Y., Matsumoto, H., 1996. Lignin deposition induced by aluminum in wheat (*Triticum aestivum*) roots. Physiol. Plant. 96, 193–198.

Scheres, B., Benfey, P., Dolan, L., 2002. Root development. In: Somerville, C.R., Meyerowitz, E.M. (Eds.), The *Arabidopsis* Book. American Society of Plant Biologists (first published on September 30, 2002; doi:10.1199/tab.0101; www.aspb.org/publications/arabidopsis/), Rockville, MD, pp. 1–18.

Schmid, M., Davison, T.S., Henz, S.R., Pape, U.J., Demar, M., Vingron, M., Schölkopf, B., Weigel, D., Lohmann, J.U., 2005. A gene expression map of *Arabidopsis thaliana* development. Nat. Genet. 37, 501–506.

Schwab, B., Folkers, U., Ilgenfritz, H., Hülskamp, M., 2000. Trichome morphogenesis in *Arabidopsis*. Phil. Trans. R. Soc. Lond. B, Biol. Sci. 355, 879–883.

Sessions, R.A., Zambryski, P.C., 1995. *Arabidopsis* gynoecium structure in the wild type and in *ettin* mutants. Development 121, 1519–1532.

Sibout, R., Eudes, A., Mouille, G., Pollet, B., Lapierre, C., Jouanin, L., Séguin, A., 2005. *Cinnamyl Alcohol Dehydrogenase-C* and *-D* are the primary genes involved in lignin biosynthesis in the floral stem of *Arabidopsis*. Plant Cell 17, 2059–2076.

Sibout, R., Eudes, A., Pollet, B., Goujon, T., Mila, I., Granier, F., Séguin, A., Lapierre, C., Jouanin, L., 2003. Expression pattern of two paralogs encoding cinnamyl alcohol dehydrogenases in *Arabidopsis*. Isolation and characterization of the corresponding mutants. Plant Physiol. 132, 848–860.

Somssich, I.E., Wernert, P., Kiedrowski, S., Hahlbrock, K., 1996. *Arabidopsis thaliana* defense-related protein ELI3 is an aromatic alcohol:$NADP^+$ oxidoreductase. Proc. Natl. Acad. Sci. USA 93, 14199–14203.

Stoop, J.M.H., Pharr, D.M., 1992. Partial purification and characterization of mannitol: mannose 1-oxidoreductase from celeriac (*Apium graveolens* var. *rapaceum)* roots. Arch. Biochem. Biophys. 298, 612–619.

Stoop, J.M.H., Williamson, J.D., Conkling, M.A., Pharr, D.M., 1995. Purification of NAD-dependent mannitol dehydrogenase from celery suspension cultures. Plant Physiol. 108, 1219–1225.

Terashima, N., Fukushima, K., 1988. Heterogeneity in formation of lignin – XI: an autoradiographic study of the heterogeneous formation and structure of pine lignin. Wood Sci. Technol. 22, 259–270.

Terashima, N., Fukushima, K., Takabe, K., 1986. Heterogeneity in formation of lignin. VIII. An autoradiographic study on the formation of guaiacyl and syringyl lignin in *Magnolia kobus* DC. Holzforschung 40 (Suppl.), 101–105.

The Multinational *Arabidopsis* Steering Committee, 2006. The Multinational Coordinated *Arabidopsis thaliana* Functional Genomics Project, Annual Report 2006. Available from: <http://www.nsf.gov/pubs/reports/2006_complete_masc_report1.pdf>.

Tobias, C.M., Chow, E.K., 2005. Structure of the cinnamyl-alcohol dehydrogenase gene family in rice and promoter activity of a member associated with lignification. Planta 220, 678–688.

Turner, S., Sieburth, L. E., 2003. Vascular patterning. In: Somerville, C.R., Meyerowitz, E.M. (Eds.), The *Arabidopsis* Book. American Society of Plant Biologists (first published on March 22, 2003; doi:10.1199/tab.0073; www.aspb.org/publications/arabidopsis/), Rockville, MD, pp. 1–23.

Whiting, P., Goring, D.A.I., 1982. Chemical characterization of tissue fractions from the middle lamella and secondary wall of black spruce tracheids. Wood Sci. Technol. 16, 261–267.

Williamson, J.D., Stoop, J.M.H., Massel, M.O., Conkling, M.A., Pharr, D.M., 1995. Sequence analysis of a mannitol dehydrogenase cDNA from plants reveals a function for the pathogenesis-related protein ELI3. Proc. Natl. Acad. Sci. USA 92, 7148–7152.

Youn, B., Camacho, R., Moinuddin, S.G.A., Lee, C., Davin, L.B., Lewis, N.G., Kang, C., 2006. Crystal structures and catalytic mechanism of the *Arabidopsis* cinnamyl alcohol dehydrogenases AtCAD5 and AtCAD4. Org. Biomol. Chem. 4, 1687–1697.

Zhang, K., Qian, Q., Huang, Z., Wang, Y., Li, M., Hong, L., Zeng, D., Gu, M., Chu, C., Cheng, Z., 2006. *Gold Hull and Internode2* encodes a primarily multifunctional cinnamyl-alcohol dehydrogenase in rice. Plant Physiol. 140, 972–983.

Zhong, R., Ripperger, A., Ye, Z.-H., 2000. Ectopic deposition of lignin in the pith of stems of two *Arabidopsis* mutants. Plant Physiol. 123, 59–69.

Zhong, R., Taylor, J.J., Ye, Z.H., 1997. Disruption of interfascicular fiber differentiation in an *Arabidopsis* mutant. Plant Cell 9, 2159–2170.